AIRBUS

DEFENCE AND SPACE

WAVEMILL

WAV-TN-ASE-012, Issue 01, Date: 12/11/2018

Wavemill Executive Summary

DRL Reference:	**N/A**	Category:	**R**
C.I. Number:	**N/A**	No. of pages:	**64**
Model:	**N/A**		

Prepared by	Revised by	Approved by
Wavemill ASE Team	**Fernando MONJAS/ Andrés SOLANA/ Ana OLEA**	**Ana OLEA**

AIRBUS

WAVEMILL

DEFENCE AND SPACE

No.:	WAV-TN-ASE-012
Issue:	01 Page: 2
Date:	12/11/2018

DISTRIBUTION LIST			
INTERNAL		EXTERNAL	
Name	**Co.**		**Name**
Wavemill ASE Team	ESA		Jean-Christophe ANGEVAIN

ISSUE RECORD					
Issue	**Date**	**Nr.**	**Chapter**	**Description of Changes**	**Impact on the Product**
01	19/09/2018	--	--	Initial Issue	

AIRBUS

DEFENCE AND SPACE

WAVEMILL

No.:	WAV-TN-ASE-012
Issue:	01 Page: 3
Date:	12/11/2018

TABLE OF CONTENTS

AIRBUS

DEFENCE AND SPACE

WAVEMILL

No.:	WAV-TN-ASE-012
Issue:	01 Page: 4
Date:	12/11/2018

FIGURES

AIRBUS

DEFENCE AND SPACE

WAVEMILL

No.:	**WAV-TN-ASE-012**
Issue:	**01 Page: 5**
Date:	**12/11/2018**

TABLES

AIRBUS

DEFENCE AND SPACE

WAVEMILL

No.:	**WAV-TN-ASE-012**
Issue:	**01 Page: 6**
Date:	**12/11/2018**

1. INTRODUCTION

This document contains the executive summary report of the Wavemill Antenna Concept and Critical Breadboarding (WAVEMILL) activities, providing a summary description of the work done during the program including a report on the analysis performed at system, antenna and breadboard level and the main results and conclusions achieved based on the Wavemill breadboard test results obtained in the frame of this program.

Based on the test results of the breadboard, an assessment of the antenna performances has also done and the conclusions are very useful for future Wavemill developments.

AIRBUS

DEFENCE AND SPACE

WAVEMILL

No.: **WAV-TN-ASE-012**
Issue: **01 Page: 7**
Date: **12/11/2018**

2. SCOPE

The scope of this Executive Summary is to summarize the activities developed in the frame of the Wavemill Antenna Concept and Critical Breadboarding ESA contract. The activities scope consists on investigate antenna architectures based on the Javelin concept for the Wavemill instrument, analyse the selected antenna configuration , define, manufacture and measure a breadboard of the critical elements for validating the antenna performances defined and assess the results obtained for the breadboard.

AIRBUS

DEFENCE AND SPACE

WAVEMILL

No.:	WAV-TN-ASE-012
Issue:	01 Page: 8
Date:	12/11/2018

3. APPLICABLE AND REFERENCE DOCUMENTS

3.1 APPLICABLE DOCUMENTS

The documents which form the customer baseline requirements and against which the data package shall be reviewed shall be identified before review data package definition:

AD	Doc. No.	Issue/ Rev.	Title
[AD01]	TEC-EEA/2011.842	1.rev 0	*Wavemill Antenna concept and critical breadboarding (SoW)*
[AD02]	ECE-O-13131_01_0	1.rev 0	*Wavemill Antenna concept and critical breadboarding (ECE PROPOSAL)*
[AD03]	ECE-WAV-BB-MOM-0002		*Negotiation Meeting Minutes*
[AD04]	ECE-WAV-BB-MOM-0003		*Technical KO Minutes of Meeting*
[AD05]			*Astrium Ltd. Mission system TN-2 contributions to : "Wavemill Antenna Breadboarding Study" Benjamin Dobke*
[AD06]			*Astrium Ltd. Mission system TN-2 contributions to : "Wavemill Antenna Breadboarding Study" Benjamin Dobke*
[AD07]	TEC-EEA/2015.2/JCA		*Memo: Wavemill Antenna Requirements.*
[AD08]	ECE-WAV-BB-MoM-0006 22/04/2015		*MoM: Wavemill Requirements Review.*
[AD09]	ECE-WAV-BB-MoM-0007 29/05/2015		*MoM: Wavemill Requirements Review.*
[AD10]	ECE-WAV-BB-MoM-0008 18/06/2015		*MoM: Wavemill Requirements Review.*
[AD11]	ECE-WAV-BB-MoM-0009 09/07/2015		*MoM: Wavemill Requirements Review.*
[AD12]	ECE-WAV-BB-MoM-0010 29/07/2015		*MoM: Wavemill Requirements Review.*
[AD13]	ECE-WAV-BB-MoM-0011 14/09/2015		*MoM: Wavemill Requirements Review.*

Table 3-1: Applicable documents.

AIRBUS

WAVEMILL

DEFENCE AND SPACE

No.:	WAV-TN-ASE-012
Issue:	01 Page: 9
Date:	12/11/2018

3.2 REFERENCE DOCUMENTS

RD	Doc. No.	Issue/ Rev.	Title
[RD01]	WM-DD-ASU-SY-0001 (issu01)		*Wavemill Instrument Design concept*
[RD02]	ECE-WAV-BB-MoM-0015. 20/04/2016		*Baseline Concept Review (MoM of Teleconference)*
[RD03]	ECE-WAV-BB-MoM-0016 22/04/2016		*BCR RIDs Review (MoM of Teleconference)*
[RD04]	ECE-WAV-BB-TN-002	02	*Wavemill Antenna Requirements*
[RD05]	ECE-WAV-BB-TN-004	01	*Wavemill Trade-off Analysis Report*
[RD06]	ECE-WAV-BB-TN-005	02.2	*Wavemill Antenna Components Requirements*
[RD07]	WVML-SE-TNO-0006 19/07/2016		*Contribution to TN-6 Antenna Design Description and justification file DRAFT5.(SPENG)*
[RD08]	ECE-WAV-BB-TN-001	03	*Wavemill: Survey of state of the art.*
[RD09]	ECE-WAV-BB-TN-006	03.4	*Wavemill Antenna design Description & justification files.*
[RD10]	ECE- WAV-BB-MoM-0017 26.10.2016		*MoM: Preliminary Concept Review (PDR)*
[RD11]	ECE-WAV-BB-TN-007	02.2	*Wavemill Preliminary Breadboard Description*
[RD12]	WAV-TN-ASE-008	01.3	*TEST PLAN OF THE ANTENNA CRITICAL ELEMENTS BREADBOARD*
[RD13]	WAV-TN-ASE-009	01	*Test Report for the antenna critical elements breadboard*
[RD14]	WAV-TN-ASE-011	01	*Wavemill Final Report.*

Table 3-2: Reference documents.

AIRBUS

DEFENCE AND SPACE

WAVEMILL

No.:	WAV-TN-ASE-012	
Issue:	01	Page: 10
Date:	12/11/2018	

3.3 ACRONYMS

ABBV	Abbreviation
AD	Applicable Document
ARR	Antenna Requirements Review
ASE	Airbus Defence&Space España.
BCR	Baseline Concept Review.
BFN	Beam Forming Network.
DDR	Design Description Review.
DUT	Device Under Test
ECE	EADS CASA Espacio
FR	Final Review
PDR	Preliminary Design Review
PRF	Pulse Repetition Frequency
RD	Reference Document.
RF	Radio Frequency
SAR	Synthetic Aperture Radar
SGH	Standard Gain Horn.
SNR	Signal Noise Relation.
SOW	Statement of Work.
RTMM	Reduced Thermal mathematical Model
TBC	To Be Confirmed
TBD	To Be Discussed.
TR	Test Report.
TRB	Test Review Board.
VNA	Vectorial Network Analyzer

AIRBUS

DEFENCE AND SPACE

WAVEMILL

No.:	**WAV-TN-ASE-012**
Issue:	**01 Page: 11**
Date:	**12/11/2018**

4. WAVEMILL FUNCTIONAL DESCRIPTION

The Wavemill is an RF instrument which follows a pure along-track interferometer concept, the 'Javelin' concept. In the Javelin concept, master and slave phase centres should be perfectly aligned in the along track direction, and the resulting interferogram, co-located, is only sensitive to surface motion.

Earlier studies resulted in an instrument design based on four separate antenna structures. This concept, whilst having good predicted performance potentially experienced differential heating across the antennas which required compensation and complicated the instrument calibration. An alternative design called 'Javelin' based on two in-line antenna structures was therefore developed which would experience a more uniform thermal environment and simplify in-orbit calibration.

4.1 FUNCTIONAL DESCRIPTION (PRINCIPLE OF OPERATION).

The Wavemill instrument calls for an antenna capable of generating up to four squinted beams with a swath of around 100km. The instrument is composed of 2 subsystems, each subsystem include 2 antennas and both fore and aft subsystem are separated by a baseline distance of more than 12 meters in the along-track direction. One single antenna shall transmit a dual linear polarized pulsed signal in one beam at a time. Each antenna of the two subsystems shall receive in a dual linear polarized mode the reflected signal within this beam. This operation shall be repeated successively 4 times, for the 4 different beams. The Javelin Wavemill instrument operation provides the required along-track interferometric baselines with a compact spacecraft at launch.

Each antenna subsystem shall be able to produce 4 transmit beams in dual linear polarization, and for each transmitted beam, the 2 antenna subsystems separated in along track shall be able to produce at the same time the same beam footprint to receive the reflected radar signal in the same polarization.

The antenna subsystem is defined as the antenna radiating aperture(s) , the feeding network, the single antenna structure, the deployment arm interconnecting the antenna to the host spacecraft, the relevant hold-down and release system, and the deployment and pointing mechanism.

The orientation of the vertical polarization shall be perpendicular to the flight direction at mid footprint incidence angle, horizontal polarization shall be orthogonal to the vertical one (See Figure 4.1).

AIRBUS

DEFENCE AND SPACE

WAVEMILL

No.:	**WAV-TN-ASE-012**
Issue:	**01 Page: 12**
Date:	**12/11/2018**
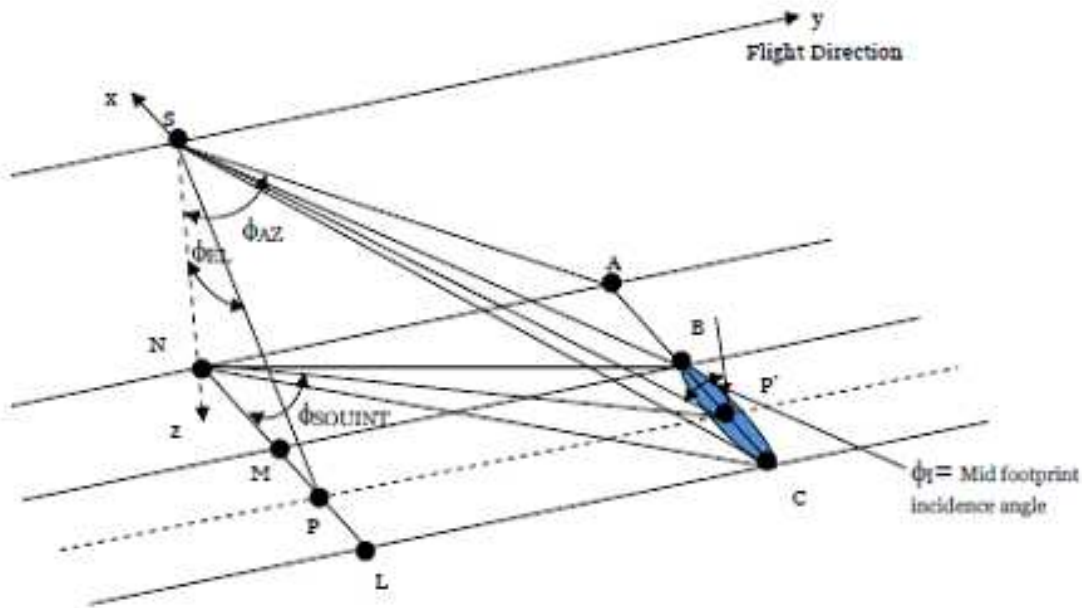
Figure 4.1 Satellite coordinate system and swath angles.

The Wavemill (Javelin) antenna system comprises two radiating subsystems separated 15 meters in the along track direction. Each of the two subsystems have to produce four beams which are squinted by 45° fore and aft to allow along and across track interferometry.

One single antenna subsystem transmits a dual linear polarized pulsed signal in one beam at a time, while both antenna subsystems receive in a dual linear polarized mode the reflected signal within this beam.

AIRBUS

DEFENCE AND SPACE

WAVEMILL

No.: **WAV-TN-ASE-012**
Issue: **01** Page: **13**
Date: **12/11/2018**
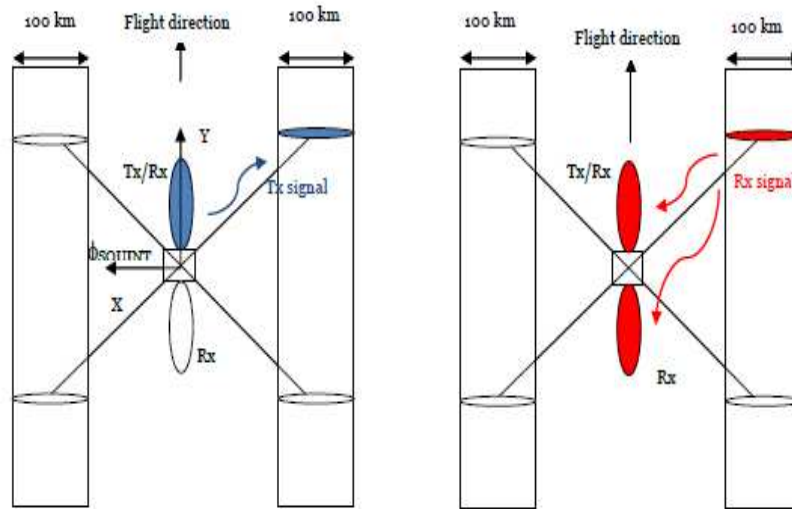
Figure 4.2 TX and RX operation modes.

4.2 ORBIT PARAMETERS.

The orbital parameters relevant to this study are:

Orbit Parameters	
Orbit Type	*Sun Synchronous*
Altitude	*500 km*

Table 4.1:

5. WAVEMILL ANTENNA REQUIREMENTS.

The consolidated requirements relevant to the Wavemill Antenna are included in the ESA Statement of Work AD[1] supersedes by the requirements included in Memo TEC-EEA/2015.2/JCA AD[7] sent by ESA on February 2015 and updated during the teleconferences for consolidation of the requirements held between ESA, ADS-UK, STARLAB, SPENG and ADS-SP AD-08, AD-09, AD-10, AD-11 and AD-12.

Therefore, some new added items which are considered to be relevant for the antenna design are also considered as required for the Wavemill antenna.

AIRBUS

DEFENCE AND SPACE

WAVEMILL

No.:	WAV-TN-ASE-012
Issue:	01 Page: 14
Date:	12/11/2018

5.1   FUNCTIONAL REQUIREMENTS.

Here below a summary of the most relevant functional requirements are included.

- Frequency of operation: Ku band (13.5 GHz).
- Beam pointing directions resulting from a system trade-off analysis between the instrument accuracy and the sea surface backscattering.

	Elevation angle ϕ_{EL}	Azimuth angle ϕ_{AZ}
Beam #1	20.3°	20.3°
Beam #2	-20.3°	20.3°
Beam #3	-20.3°	-20.3°
Beam #4	20.3°	-20.3°

Table 5.1: Beam pointing direction.

- Given a satellite altitude of 500 km, the antenna elevation pattern must present a slope equal to 0.139dB/deg, to compensate for the two-way path loss in the beam footprint. Besides, to avoid range ambiguities, the side-lobes in elevation plane must be kept as low as possible because of the danger of returns from the swath in opposite side → the required directivity mask in elevation plane of the two beams pointing on the right satellite side
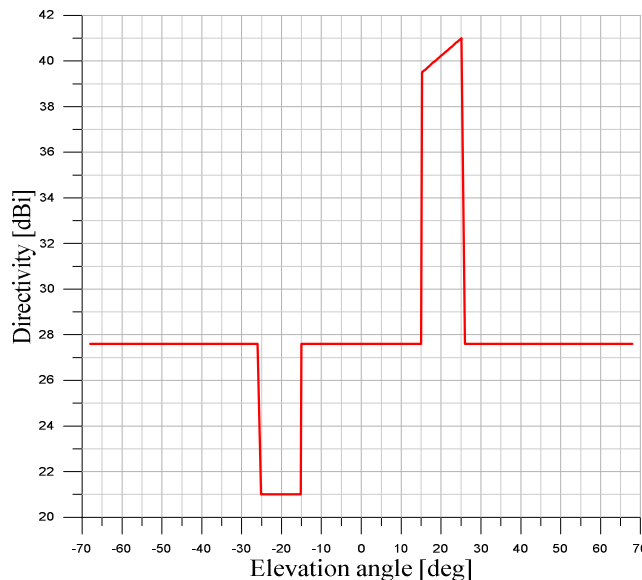

Figure 5.1 Directivity mask in elevation plane.

AIRBUS

DEFENCE AND SPACE

WAVEMILL

No.:	**WAV-TN-ASE-012**
Issue:	**01 Page: 15**
Date:	**12/11/2018**

- To match this directivity mask and a directivity of 41 dB, the across and along-track beam-widths must be around 9.9° and 0.17° respectively, obtainable at 13.5 GHz by <u>long</u> aperture of size 0.2 meters in elevation x 7.0 meters in azimuth.

5.2   POLARIZATION ISSUES

The Wavemill instrument needs the radar echoes relative to the horizontal (E_{TE}) and vertical (E_{TM}) polarizations on the sea surface (see Fig.5.2). As a squinted beam induces a rotation of the E-field components, the two linear polarizations radiated by the antenna have to be tilted on the aperture plane by specific angles which depend on the direction of the squinted beam and the antenna positioning on board the satellite.
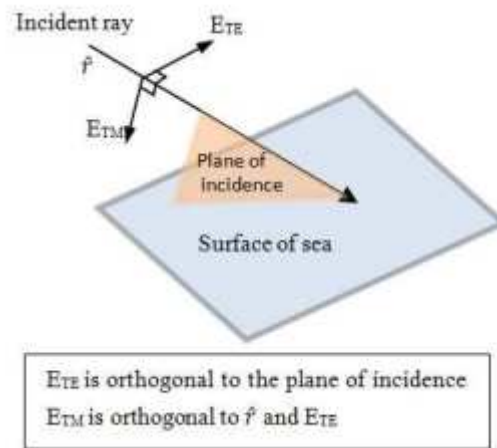
Figure 5.2   Definition of E_{TM} and E_{TE}.

For an antenna pointing to the nadir (flat antenna arrangement), the two polarization inclinations on the antenna aperture to generate radiated field aligned with E_{TE} and E_{TM} on the swath centre result exactly equal to ±45° with respect to the satellite flight direction. Next figure shows the relative cross-polar values along the swath angular region expressed in satellite reference system.
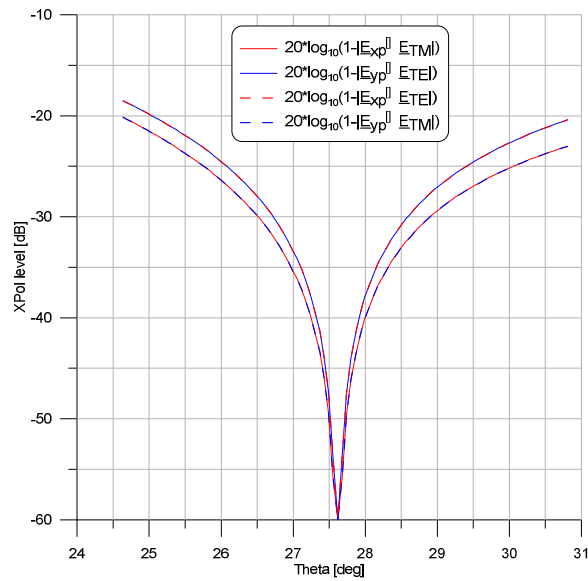
AIRBUS

DEFENCE AND SPACE

WAVEMILL

No.:	WAV-TN-ASE-012
Issue:	01 Page: 16
Date:	12/11/2018

Figure 5.3 Cross-polar along the swath.

AIRBUS

DEFENCE AND SPACE

WAVEMILL

No.:	**WAV-TN-ASE-012**
Issue:	**01 Page: 17**
Date:	**12/11/2018**

6. ANTENNA SUITABLE CONCEPT

The Wavemill oceanographic radar is an instrument intended to measure ocean current speed, direction and wave height over a wide coverage area (100 km swaths).

The measurements are made on four illuminated areas, left and right and fore and aft of the sub-satellite track. A total of four beams are generated (dual polarization). The antenna pairs need a relative phase centre displacement of 15 meters.

Two concepts were studied:

- Classical rooftop concept with four antenna apertures boresight pointed to each squinted beam.
- Javelin in-line concept with two antenna apertures oriented broadside to the sub-satellite track. Selected due to accommodation and complexity and thermal reasons (no differential heating between antenna structures).
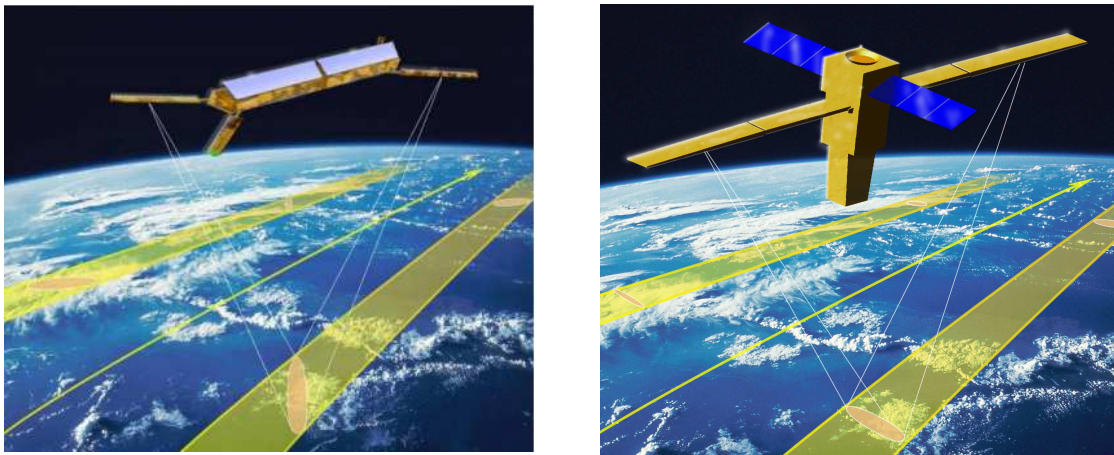

Figure 6.1 Rooftop concept and Javelin in-line selected concept.

Rooftop configuration allows pointing the beams to the desired elevation direction so it does not need to steer the beam in elevation. On the contrary, it requires two apertures, one per beam in elevation so it is heavier than flat configuration. Flat configurations can use one or two apertures to generate both right and left beams.

Flat configuration implies a small directivity loss due to the reduction of the antenna projected aperture (around 0.2 dB for the required elevation pointing around 20°) but grating lobes elevation effect can be controlled in both rooftop and flat configurations.

Flat configuration offers a more compact design in stowed configuration. Much more complex structure and HRM design for rooftop is expected, which also implies more mass. Also designs to cope with thermo-elastic distortions are more complex for rooftop configurations.

AIRBUS

WAVEMILL

DEFENCE AND SPACE

No.:	**WAV-TN-ASE-012**
Issue:	**01 Page: 18**
Date:	**12/11/2018**

The main difference between flat and rooftop configurations are related to thermal issues that appears for rooftop configurations as sun illumination may be different in the different parts of the antenna, mainly between fore and aft antennas. Due to the azimuth pointing sensitivity it is very important to minimize temperature gradients between fore and aft antennas, which is very difficult to achieve for rooftop configurations.

7.   WAVEMILL ANTENNA CONFIGURATION.

The antenna configuration selected for the tow radiating subsystems is the end-fed slotted-waveguide planar array. This well-established solution besides giving advantages for stowage and deployment allows a design based on the Javelin concept, i.e. with two in-line antenna subsystems pointing to the nadir, so as to avoid differential heating across the antenna due to the solar flux. To fit the 7m planar arrays into the launcher, each radiating subsystems is composed of 2 folding panels of 3.5m as sketched in next figure.
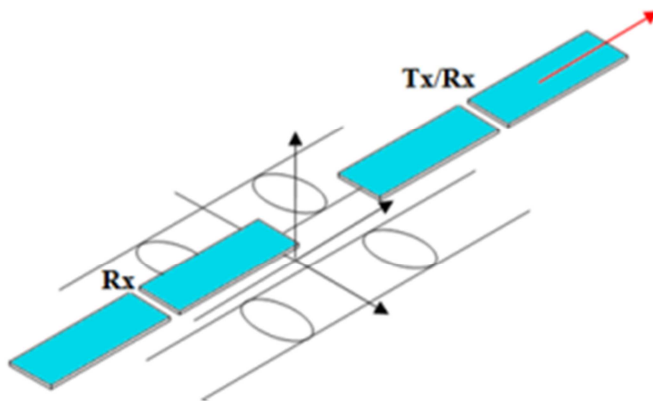

Figure 7.1 Javelin concept with folding subsystems.

The generation of the squinted beams with tilted polarizations forces the use of a particular end-fed slotted-waveguide structure: the Leaky-Wave Planar Array (LWPA), radiating through closely spaced non-resonant slots inclined by 45º.

AIRBUS

DEFENCE AND SPACE

WAVEMILL

No.: **WAV-TN-ASE-012**
Issue: **01** Page: **19**
Date: **12/11/2018**

Figure 7.2: Leaky-wave planar array.

Since power is radiated continuously along the length, the aperture field of a leaky-wave array with uniform geometry has an exponential decay. The radiation efficiency is maximized when roughly 90% of the waveguide input power is radiated. Besides, the beam squint angle depends on ratio of free space an waveguide wavelength.

Figure below shows the field distribution along the 7 meter LWPA made with tow 3.5 meter sub-array panels.
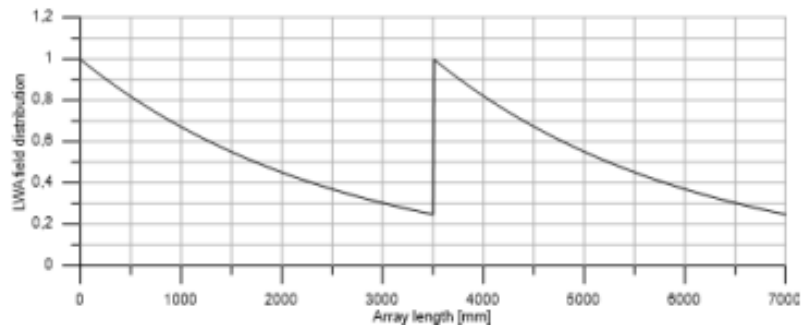

Figure 7.3: Field distribution along the 7 meter LWPA.

This particular field distribution produces the LWPA azimuth pattern reported in next Figure.

AIRBUS

DEFENCE AND SPACE

WAVEMILL

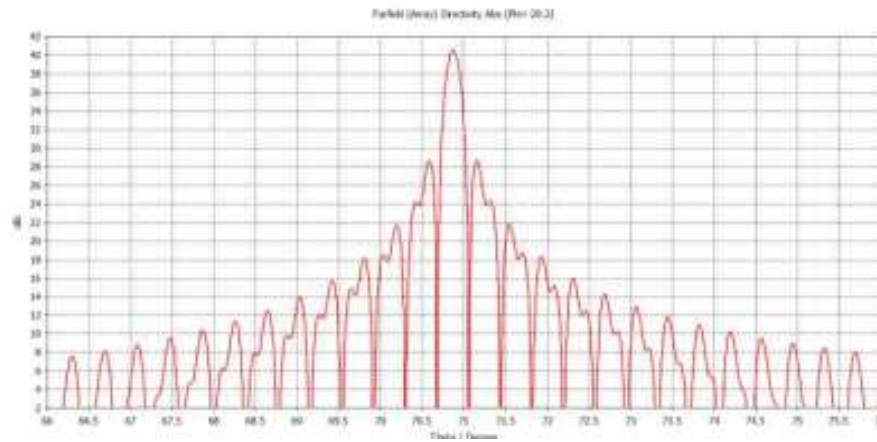| No.: | **WAV-TN-ASE-012** |
| Issue: | **01   Page: 20** |
| Date: | **12/11/2018** |

Figure 7.4: Azimuth pattern of the 7 meter LWPA.

The rather elongated shape of the LWPA makes this radiating structure practically similar to a linear distribution of small sources with linear excitation phases. Thus, the radiation solid of the array tends to extend on a cone surface, as shown in Fig.10 relative to a 7m single waveguide leaky-wave array.
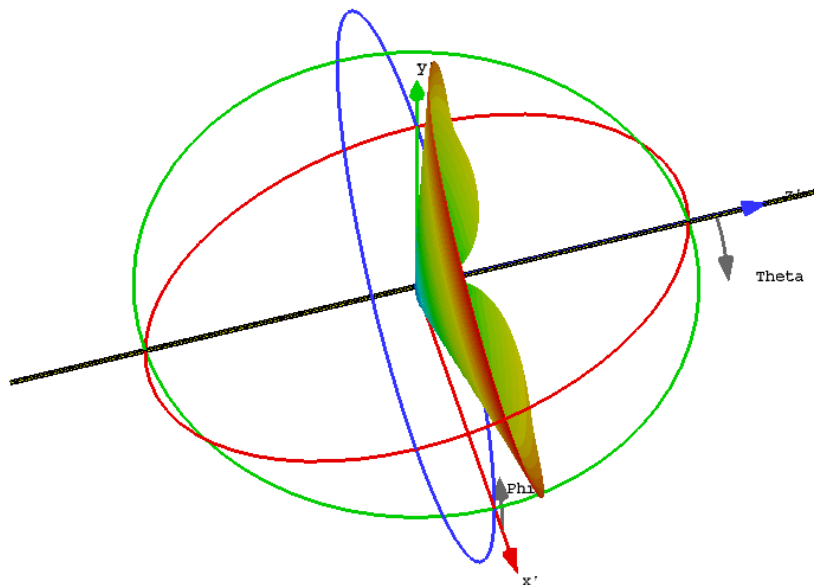

Figure 7.5: Radiation solid of a slotted waveguide..

For $\phi_{AZ} = \phi_{EL} = 20.3°$, the cone semi-vertex angle θ_{LWA} results :

AIRBUS

DEFENCE AND SPACE

WAVEMILL

No.:	**WAV-TN-ASE-012**
Issue:	**01 Page: 21**
Date:	**12/11/2018**

$$\theta_{LWA} = \cos^{-1} \frac{\tan \Phi_{AZ}}{\sqrt{\frac{1}{\cos^2\Phi_{EL}} + \tan^2\Phi_{AZ}}} = 70.867°,$$

Corresponding to a squint angle of 90º- θ_{LWA} = 19.133º respect to the broadside axis. This squint angle, resulting from the system trade-off is quite close to the limit value of about 15º due to the waveguide cut-off. Consequently, the LWPAs suffer from ohmic losses not negligible and from a beam-pointing sensitivity to manufacturing tolerances.

The LWPA can be fed independently from either ends generating plus and minus squint angles as required by Wavemill. This, in principle, makes it possible to irradiate the 4 squinted beams in the two opposite linear polarizations, here simply referred as 4H and 4V, using a single aperture made of two 3.5m panels with interleaved dual-ended LWPAs (see Fig.7.6 and Fig.7.7)

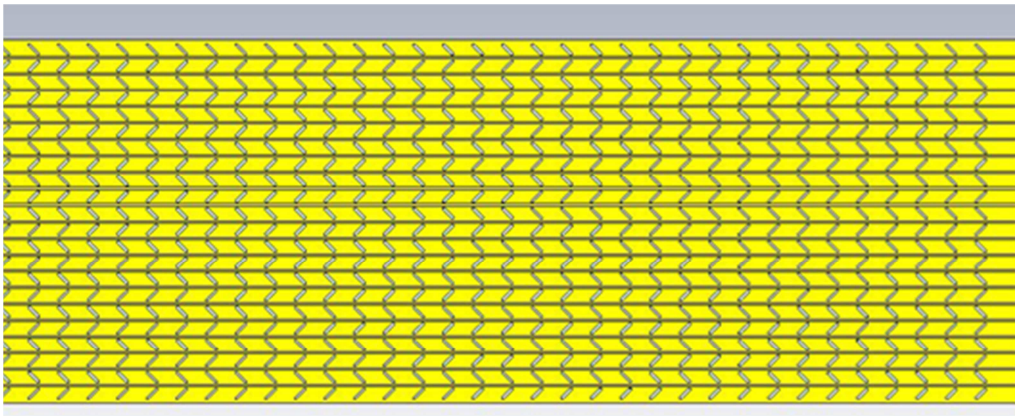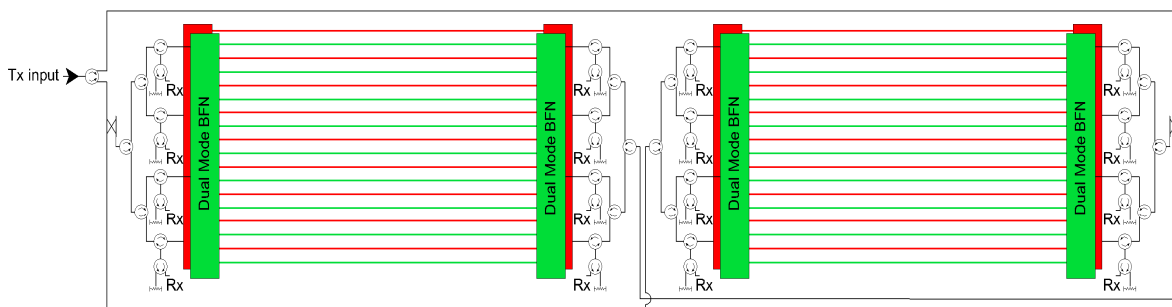**Figure 7.6:particular of two interleaved LWPAs.**

Figure 7.7:Tx/Rx aperture radiating 4H+4V beams.

The configuration sketched in Fig.7.7 shows the two array panels where the slotted waveguides of the interleaved arrays are represented with red and green lines. The generation of the beams that are symmetrical to the satellite direction is obtained by using a dualmode network, which is able to

AIRBUS

DEFENCE AND SPACE

WAVEMILL

No.:	WAV-TN-ASE-012
Issue:	01 Page: 22
Date:	12/11/2018

provide the necessary amplitudes and phases by virtue of the orthogonality between these two beams.

However, due to the aforementioned sensitivity to manufacturing tolerances and the stringent beam coalignment requirements (around 0.01º), the solution of Fig.7.7 has been discarded in favour of one with 4 separate apertures allowing independent azimuth pointing, which is not feasible with dual-ended array configurations. Also interleaved polarizations configurations are discarded due to pointing and manufacturing issues and degraded performances. Fig.7.8 shows the selected subsystem configuration with four apertures able to generate the 4H+4V instrument beams.
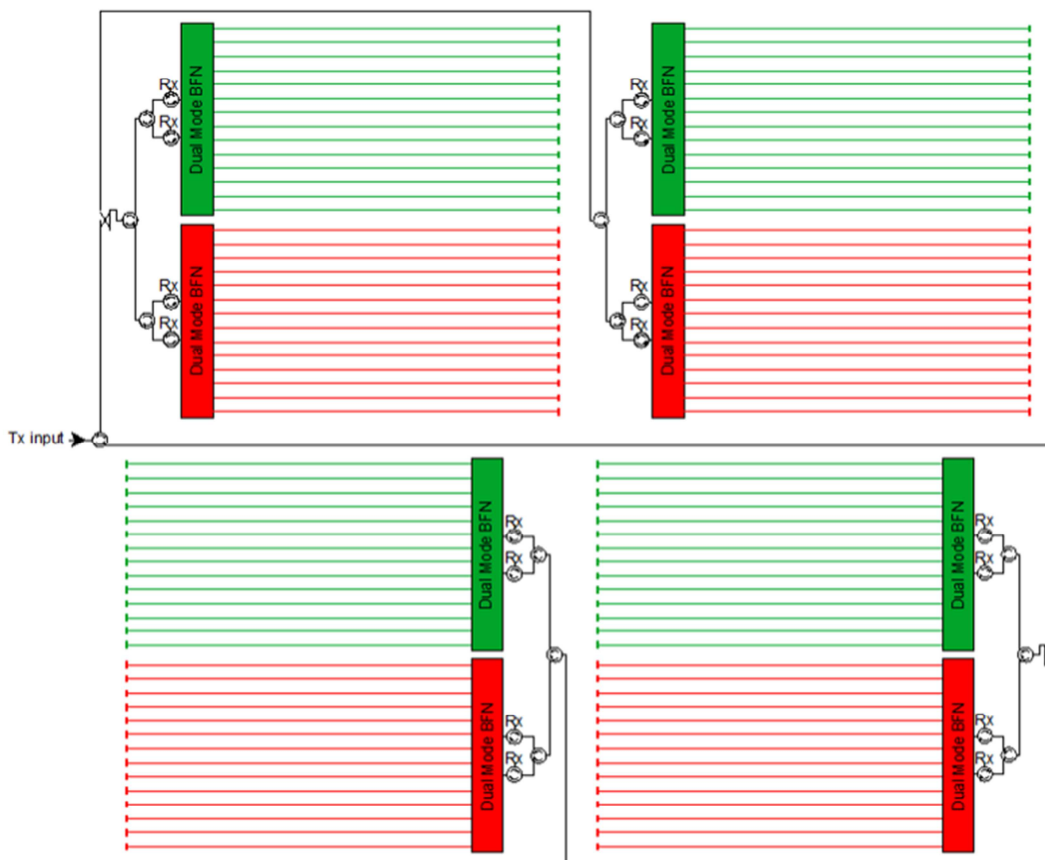

Figure 7.8: Four 7m apertures radiating 4H+4V beams.

A basic scheme of a 2in/12out dual-mode network showing the required unbalanced Power Divider (PD) and fixed Phase Shift (PS) is depicted in next figure. The realization of this network in bar-line technology enables a significant saving of its mass and volume.
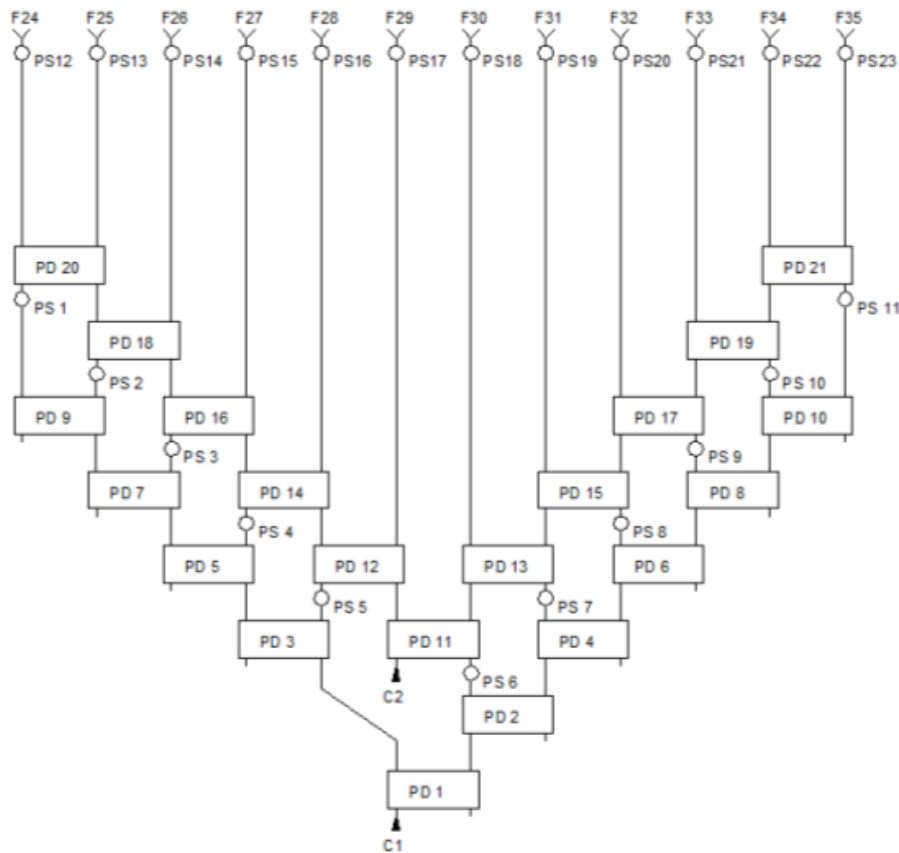
AIRBUS

DEFENCE AND SPACE

WAVEMILL

No.:	WAV-TN-ASE-012
Issue:	01 Page: 23
Date:	12/11/2018

Figure 7.9: 2in/12out dual-mode network.

7.1   ANTENNA ELECTRICAL DESIGN DESCRIPTION.

The two arrays radiating the same beam with opposite linear polarizations have a different slot orientation respect to the beam direction. Consequently, their radiation solids exhibit differences in the swath region that must be reduced as much as possible. Fig.7.10 shows the active pattern of the slotted waveguide in the central position of the 7m LWPA depicted in Fig.7.6 and obtained by full-wave analysis. The pattern drop for positive phi values can be brought out of the swath angular region 15.17°÷25.07° by adjusting properly the separation between the planar array slotted waveguides. A spacing of 14.5mm allows a nearly flat pattern in the angular region -25.7°÷ +25.7°, so enabling the synthesis of closely identical instrument beams.

AIRBUS

DEFENCE AND SPACE

WAVEMILL

No.:	WAV-TN-ASE-012
Issue:	01 Page: 24
Date:	12/11/2018
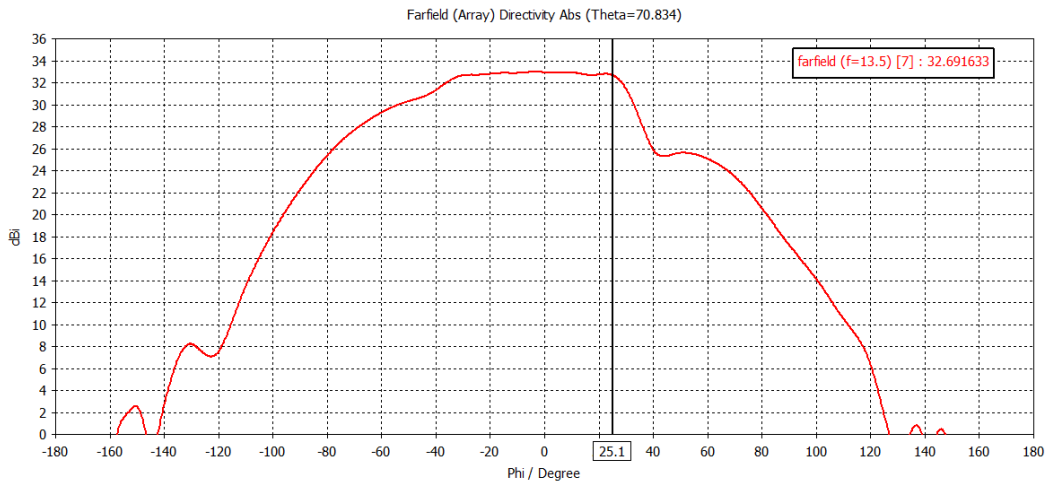
Figure 7.10: Active pattern of an inner slotted waveguide.

On the basis of a further trade-off analysis, the optimum number of slotted waveguides for each LWPA has also been determined. Considering both the attainable electrical performance and the mass and volume characteristics associated with the various solutions, a number of 12 slotted waveguide for each LWPA has been fixed. Then, a synthesis of the shaped elevation pattern has been performed based on the active pattern of each slotted waveguide. The result is presented in Figure 7.11 which shows a very small deviation between the calculated shaped beam and the required directivity mask.

AIRBUS

DEFENCE AND SPACE

WAVEMILL

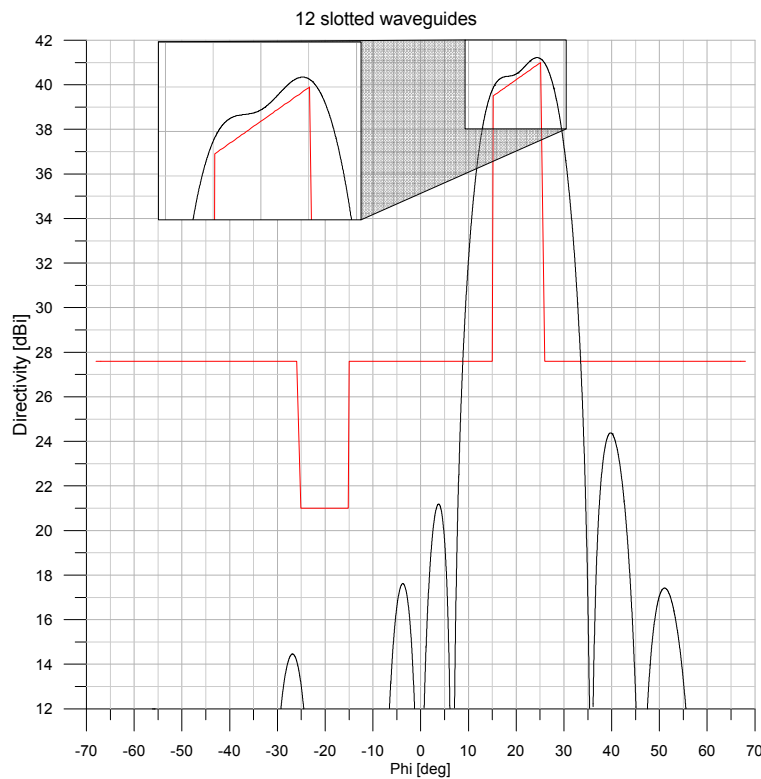| No.: | **WAV-TN-ASE-012** |
| Issue: | **01   Page: 25** |
| Date: | **12/11/2018** |

Figure 7.11: Shaped beam for a 12-WGs LWPA

Table 7.1 reports the gain budget of the 12-WG LWPA in the angular direction corresponding to the swath far point. Part of the losses is due to the waveguide feeding system of the two panels which, in addition to providing identical excitation amplitudes at the panel inputs, must also ensure the continuity of the phase-front along the whole radiating aperture. Due to this last aspect the waveguide feeding the most distant panel must have the same cross section of the slotted waveguides, thereby implying a significant ohmic loss.

	Wavemill Antenna
Directivity of the 7m array	41.16 dBi
Total efficiency of the 7m array	-1.86 dB
Efficiency of the feeding system of the 2 array panels (Ppanel_1+ Ppanel_2 / |S21|2 =1)	-1.09 dB
Realized Gain	**38.21 dBi**

Table 7.1: Gain performance of baseline antenna at the swath far point

AIRBUS

WAVEMILL

DEFENCE AND SPACE

No.: **WAV-TN-ASE-012**
Issue: **01 Page: 26**
Date: **12/11/2018**

7.2 THERMAL DESIGN & PERFORMANCES.

The main objective of the Wavemill antenna thermal design is to provide well controlled temperatures for all elements, ensuring low thermal distortions and low dispersion among the different areas of the antenna.

To evaluate the thermal design a dedicated thermal model has been created (Fig.7.12). It contains the spacecraft body, the foldable bars and the antennas themselves. They are composed of the Boom, the Radiating Elements and the Structure. RF dissipations have also been included in the computations. The effect of foldable bars is limited in terms of waveguides temperatures. The fact of having white finish for waveguides, increases its capability of heat rejection minimising gradients encountered due to RF dissipation.
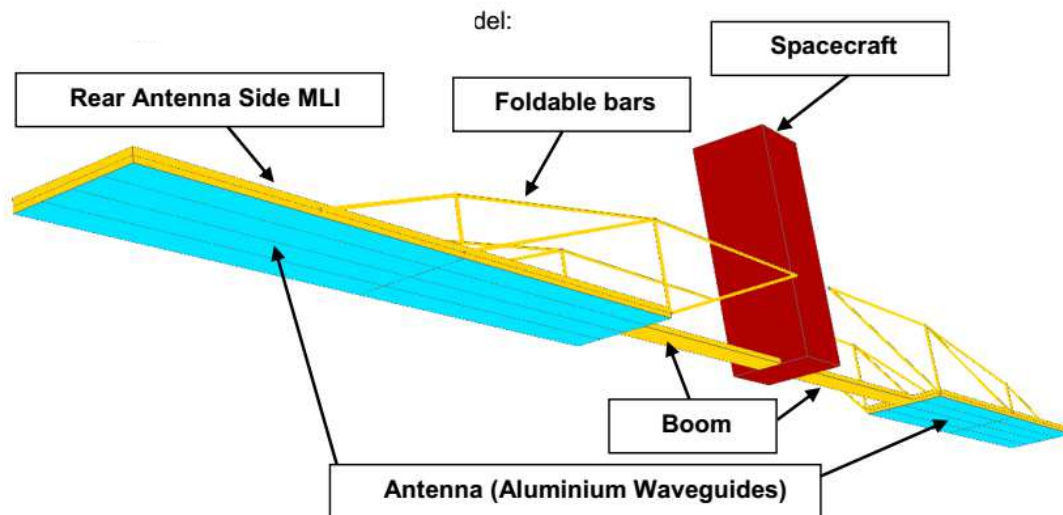

Figure 7.12: Wavemill thermal design.

For this preliminary design, two different thermal designs have been considered: a first one based on aluminium tape, and a second one based on white paint finish for the antenna front face. In both proposals the rear face of the antenna is isolated from the environment by means of a higher efficiency MLI (4 layers Kapton MLI).

The temperatures in all the cases are close to the assembly temperatures. Ranges are narrow enough to absorb margins, uncertainties and new power dissipation values.

For both finishes maximum temperatures are reached in 00 a.m. orbit. Low α/ε ratio of white paint contributes to reach lower maximum temperatures. High emissivity of white paint reduce dissipation influence on gradients. Tables below take into account the dissipation on the fore antenna.

AIRBUS

DEFENCE AND SPACE

WAVEMILL

No.:	WAV-TN-ASE-012
Issue:	01 Page: 27
Date:	12/11/2018

Gradients (Al tape)	Grad Al_Tape6PM		Grad Al_Tape8PM		Grad Al_Tape10PM		Grad Al_Tape00AM	
Elements	Min [ºC]	Max [ºC]	Min [ºC]	Max[ºC]	Min[ºC]	Max [ºC]	Min [ºC]	Max [ºC]
Antenna_WG:RX_Antenna	10.6	10.7	10.6	10.8	9.1	9.2	9.0	9.1
Antenna_WG:TX_Antenna	5.6	5.6	4.8	4.9	3.8	3.9	3.9	3.9

Gradients (White paint)	Grad WhitePaint_6PM		Grad WhitePaint_8PM		Grad WhitePaint_10PM		Grad WhitePaint_00P	
Elements	Min [ºC]	Max [ºC]	Min [ºC]	Max[ºC]	Min[ºC]	Max [ºC]	Min [ºC]	Max [ºC]
Antenna_WG:RX_Antenna	1.5	1.6	1.5	1.6	1.3	1.4	1.2	1.3
Antenna_WG:TX_Antenna	2.9	3.0	2.7	2.8	2.4	2.6	2.3	2.5

Table 7.2: Gradients between Fore and Aft Antenna

Gradients for white coating are sensible lower than Al tape due to differences in emissivity values. Maximum gradients have been observed in 6PM orbit. The reason why maximum gradients appear in 6PM ascending node position is the radiative coupling between guides located closer to the edge, and the MLI covering the border. This effect could be confirmed once the orbit is fixed. MLI border effect could be reduced installing high efficiency MLI on that edge (12 layers). Baseline coating from the thermal point of view is white finish.

The thermal design is flexible enough to absorb modifications in mission, geometry materials
Another thermal design based on Sunshield to avoid direct solar fluxes in the front face of the antenna waveguides and dump temperatures excursions along the orbit is possible to face harder requirements

AIRBUS

DEFENCE AND SPACE

WAVEMILL

No.:	**WAV-TN-ASE-012**
Issue:	**01 Page: 28**
Date:	**12/11/2018**

7.3 ANTENNA MECHANICAL DESIGN & PERFORMANCES.

The mission will use a typical Earth observation platform being the challenging aspect to pack It inside the launcher fairing, due to the 22m full span of the antenna.
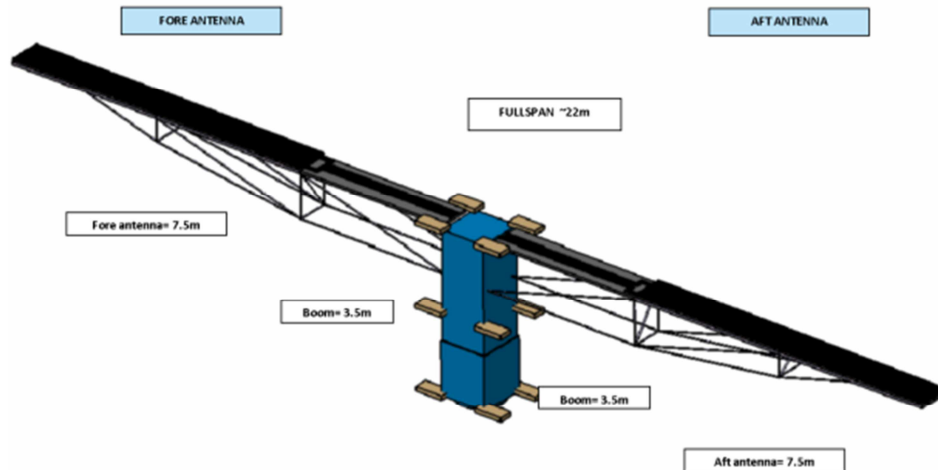
Figure 7.13 Wavemill antenna.

Phase centres of fore and aft antennas must have a separation driven by RF design This separation is achieved by means of a boom, 3.5 m long. The span of a one side assembly reaches then 11 m of length.
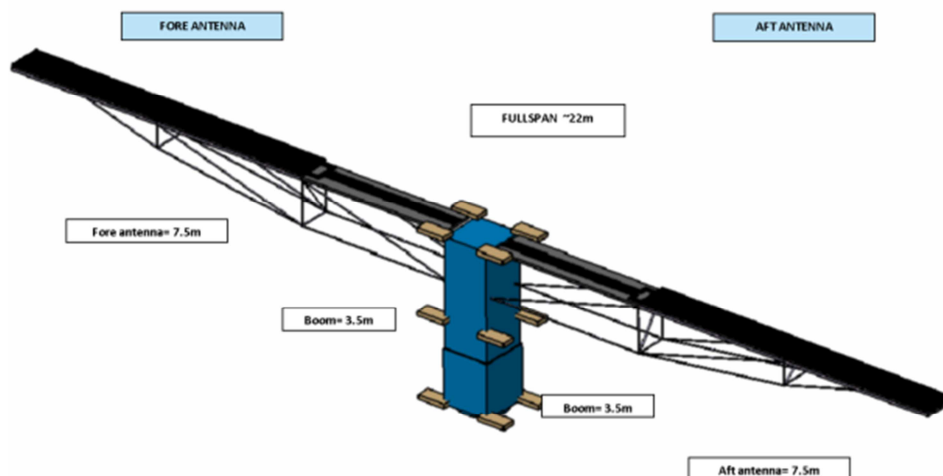
Figure 7.14 Wavemill antenna length.

AIRBUS

DEFENCE AND SPACE

WAVEMILL

No.:   **WAV-TN-ASE-012**
Issue: **01**   **Page:**   **29**
Date: **12/11/2018**

The first mechanical challenge for this mission is to pack both antennas inside the fairing of the launcher. Figure below shows the Wavemill antenna deployment
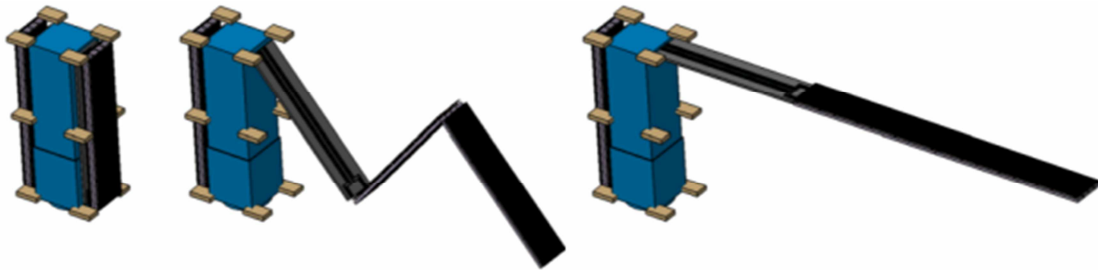

Figure 7.15 Wavemill antenna deployment.

The adopted solution is to fold the antenna around 3 hinge lines, one between the middle part of the radiating elements, other between boom and radiating elements and the last between boom and the interface with the spacecraft.
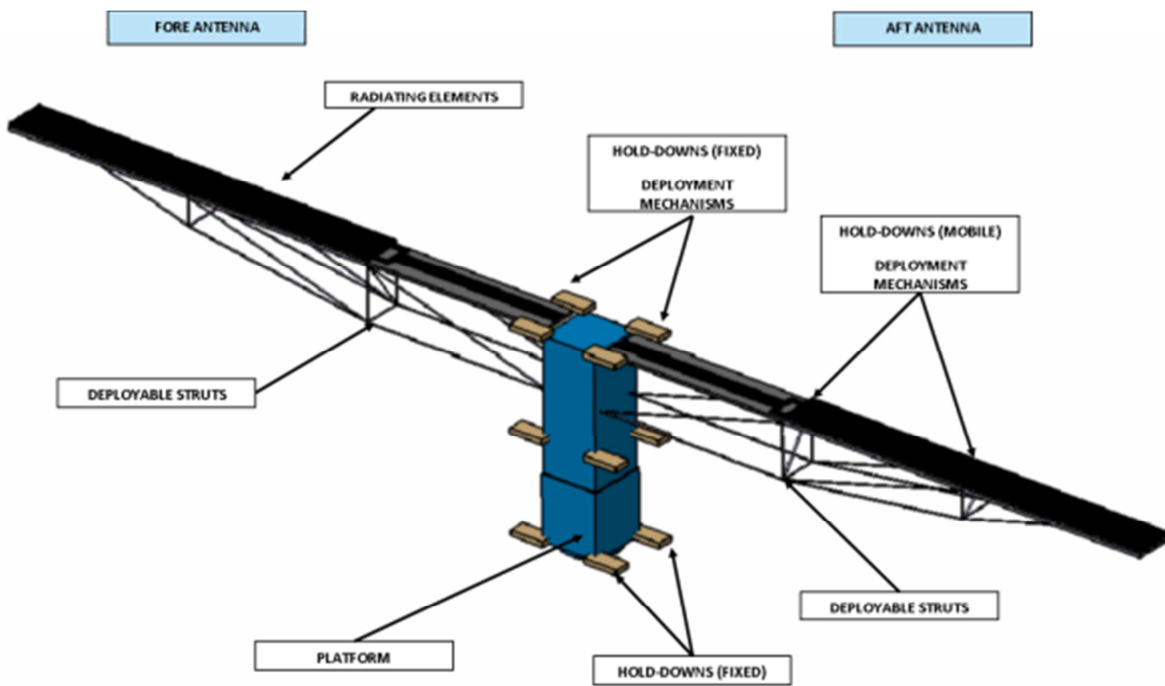

Figure 7.16 Wavemill antenna components.

The foreseen nominal launcher is Vega-C, which is an evolution of Vega that will replace it by 2020. The payload capability of Vega-C is of 2000 Kg@800Km, with increased fairing diameter and height.
Wavemill antenna is folded so as to fit inside Vega (and Vega-C) launcher fairing.
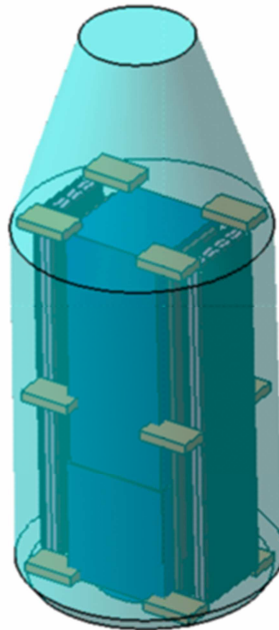
AIRBUS

WAVEMILL

DEFENCE AND SPACE

No.:	**WAV-TN-ASE-012**
Issue:	**01 Page: 30**
Date:	**12/11/2018**

Figure 7.17 Wavemill antenna inside Vega-C

Fore and aft antenna share the same mechanical design, which comprises the following elements: Boom, Support Panels (Panel 1 and 2), Isostatic Blades, Radiating elements, Beam forming networks, dividers, switches, wave guides, hold-down and release mechanisms, deployment mechanisms, and rotary joints
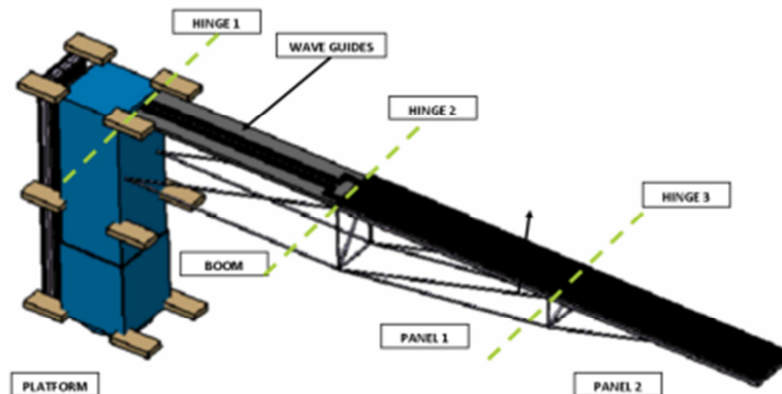

Figure 7.18 Wavemill antenna hinges lines

AIRBUS

DEFENCE AND SPACE

WAVEMILL

No.:	**WAV-TN-ASE-012**
Issue:	**01 Page: 31**
Date:	**12/11/2018**

The boom structure is a sandwich panel of CFRP skins and Aluminum honeycomb core (thickness 60 mm), which provides the separation between the fore and aft antennas phase centers and supports the RF waveguides.

This material configuration leads to an excellent mass to stiffness ratio and reduces the error in phase center distance due to thermal gradients between fore and aft antenna.

The radiating elements are supported by structural panels made with aluminum skins and aluminum honeycomb (core thickness 60 mm). The rationale for using aluminum is to have very good CTE compatibility between the support panels and the radiating elements. In this way the thermal distortions and stresses are minimized in the radiating elements
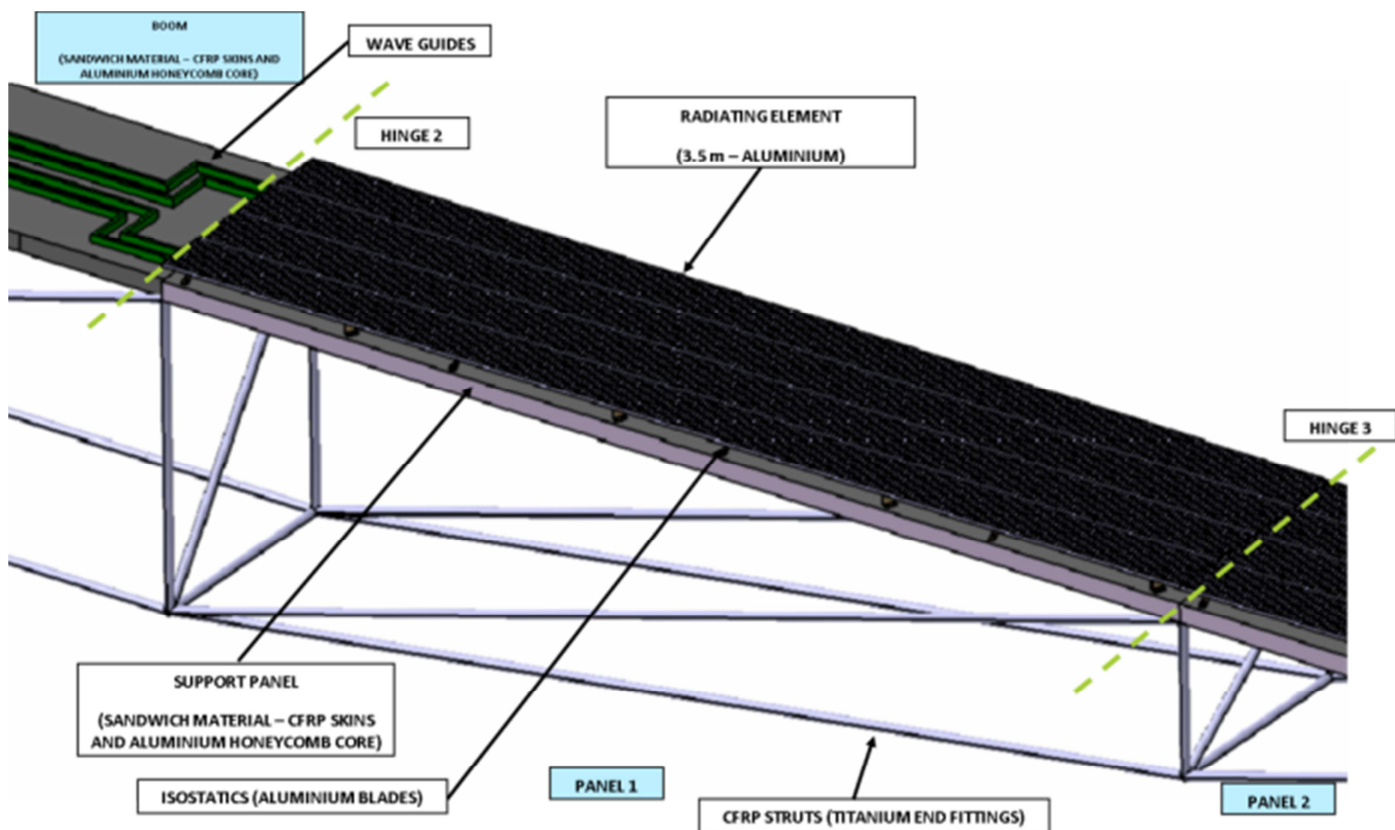

Figure 7.19 Wavemill antenna. Panels and hinges.

In general, all RF components are of aluminum alloy. Waveguides are standard extruded tubes and the radiating elements. Radiating elements are 3.5 meters length and have an average stiffness of the outside walls of 1 mm to minimize mass. Waveguides are machined or extruded along the length of the radiating element and the radiating face is populated with the radiating slots. Rotary joints are used in order to allow the rotation taking place in the deployment sequence.

A mass estimation has been performed for the WM antenna, with an added system level uncertainty of 20%. It can be seen that the antenna design is complaint with Vega-C.

AIRBUS

DEFENCE AND SPACE

WAVEMILL

No.:	WAV-TN-ASE-012
Issue:	01 Page: 32
Date:	12/11/2018

	MASS [Kg]	
	Nominal	+20%
Service Module	740	888
Payload (deployable antena not included)	110	131
DRY TOTAL		1019
prop+res+press+adapter		177
WET TOTAL		1196
Deployable antennas (Fore+Aft)	552	662
TOTAL		1859
VEGA C- capacity		2000

Table 7.3: Mass estimation vs launcher payload.

7.3.1   MECHANICAL PERFORMANCES.

7.3.1.1 STOWED CONFIGURATION.

In stowed configuration, each side of this appendage consists of three elements (approximately 3.5 m x 0.75m each one) put together. Due to the architecture of this antenna, the holding points can only be positioned along the perimeter of the stowed assembly. At least six holding points are foreseen per side to obtain a first frequency between 23Hz and 47Hz depending on the final achievable HRM (i.e. Holding and Release Mechanism) stiffness.
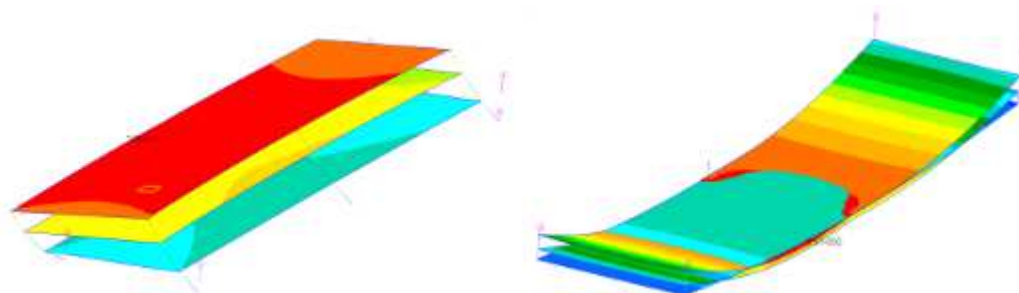

Figure 7.20 : Low HRM stiffness first eigen-modes (f>23Hz)

AIRBUS

DEFENCE AND SPACE

WAVEMILL

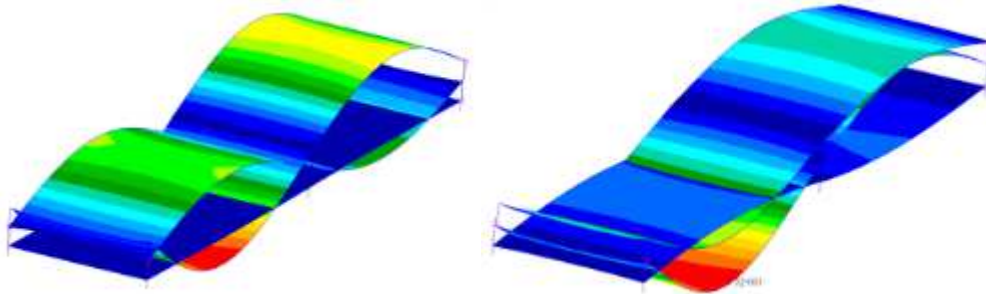| No.:	**WAV-TN-ASE-012**	
Issue:	**01**	**Page: 33**
Date:	**12/11/2018**	

Figure 7.21 High HRM stiffness first eigen-modes (f<47Hz)

This kind of construction in which each HRM holds together the three stacked panels to the platform is common for large deployable appendages (e.g. SAR,solar panels) as it minimizes the number of holding mechanisms.
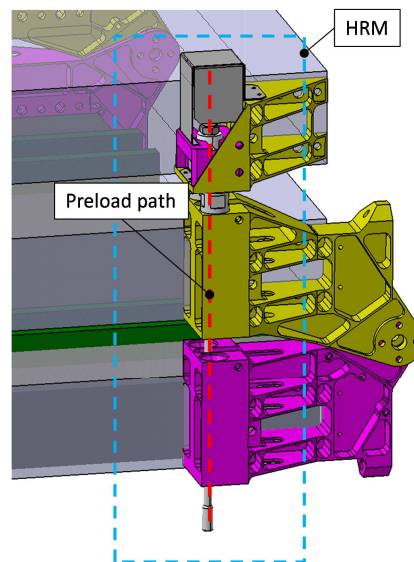

Figure 7.22 Panels stacked and held by the HRMs (from SMOS mission).

7.3.1.2 DEPLOYED CONFIGURATION.

The proposed architecture to be deployed does not differ much from previous missions part from the higher mass and inertia.

Due to this, taking advantage of Airbus DS Spain experience acquired on SMOS mission, a flat and synchronized deployment like the one implemented in this mission is selected as the best solution to adopt. The synchronization system consists of several pulleys at each hinge which are linked by means of cables. By adjusting the diameter of these pulleys a defined rate between deployed angles per panel is guaranteed. The main advantages of this solution are:

AIRBUS

DEFENCE AND SPACE

WAVEMILL

No.: **WAV-TN-ASE-012**
Issue: **01** Page: **34**
Date: **12/11/2018**

- Flat deployment allowing easy on-ground testing.
- Pure mechanical deployment. Speed regulator and synchronization by means of cables provide a safe and repeatable deployment.
- Already flying mission in a smaller size (~4m length).

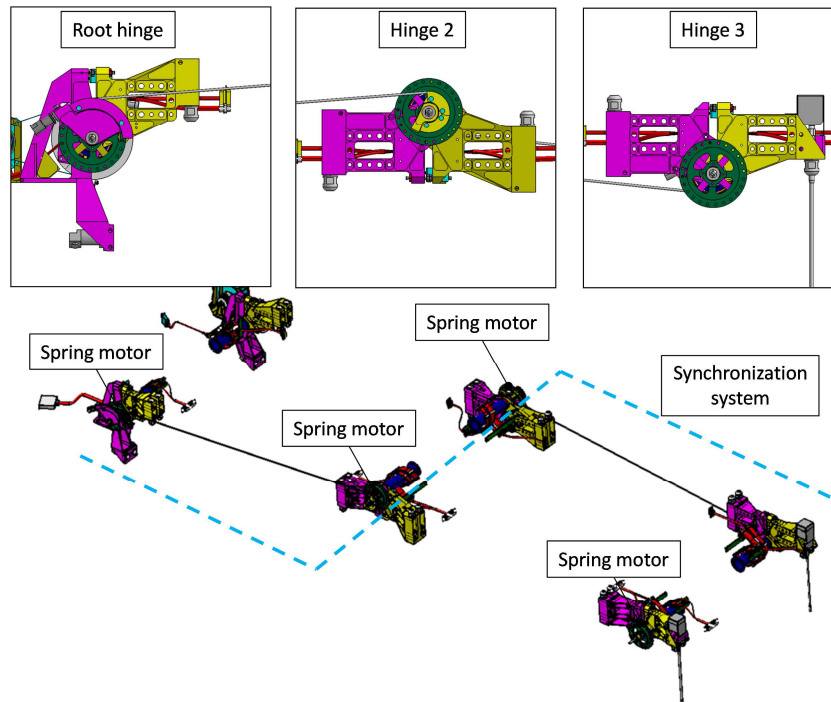**Figure 7.23 SMOS deployment system.**

Key point of this deployment to highlight are driven by the high inertia of each appendage, which is nearly 13000 kg·m^2 at root level for the baseline design. Future studies will have to trade adequate engineering concepts to cope with the main effects of this, like the high values foreseen for the torques derived at the speed regulator and end of the deployment.
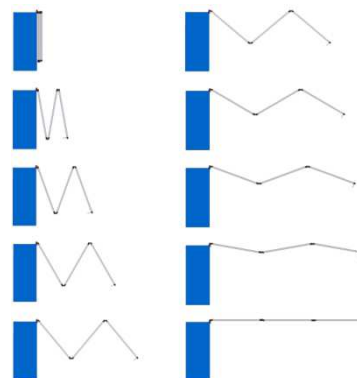
AIRBUS

WAVEMILL

DEFENCE AND SPACE

No.: **WAV-TN-ASE-012**
Issue: **01** Page: **35**
Date: **12/11/2018**

Figure 7.24: Synchronized deployment sequence

A study has been carried out from the stiffness point of view of the deployed configuration. The antenna design, which schematically consists of three beams (sandwich panels) joint together by torsional springs (mechanisms torsional stiffness) shows a first frequency of 0.16Hz.

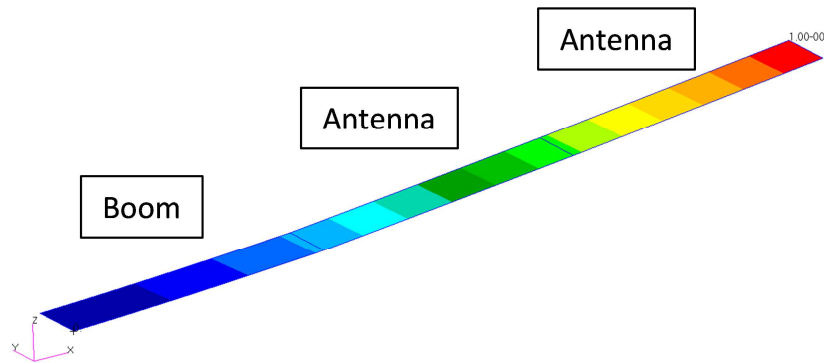**Figure 7.25: Deployed first eigen-mode shape (boom + antenna + antenna)**

The modal response gives the first frequency modes well above the classic requirement from AOCS (1.5Hz)

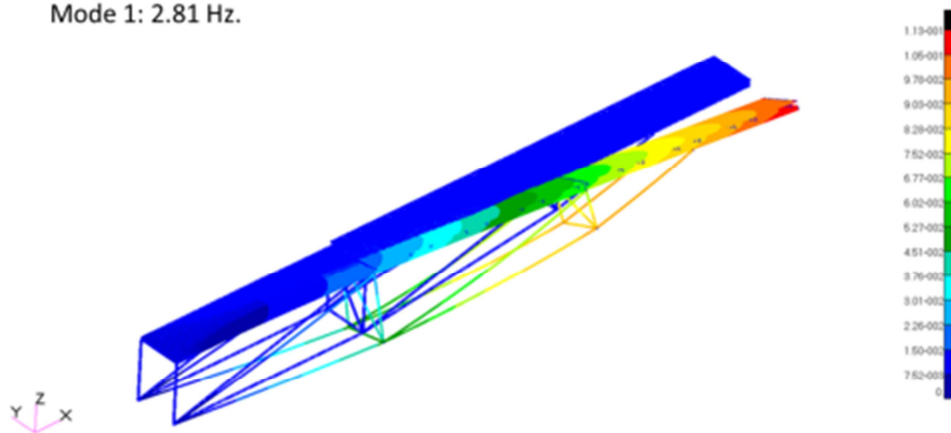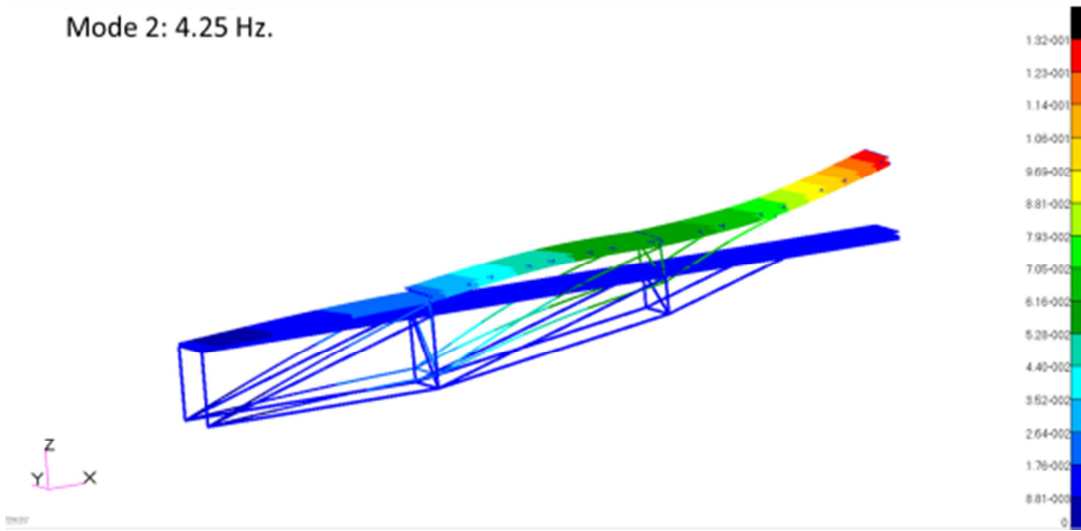**Figure 7.26: Deployed first eigen-mode shape**

AIRBUS

DEFENCE AND SPACE

WAVEMILL

No.:	**WAV-TN-ASE-012**
Issue:	**01 Page: 36**
Date:	**12/11/2018**

Figure 7.27:: Deployed second eigen-mode shape

AIRBUS

DEFENCE AND SPACE

WAVEMILL

No.:	**WAV-TN-ASE-012**
Issue:	**01** Page: **37**
Date:	**12/11/2018**

8. WAVEMILL BREADBOARD DESCRIPTION

Wavemill breadboard has been designed, manufactured and tested in order to validate the RF design and technology of the Wavemill antenna.

Wavemill breadboard model consists of the following main blocks:

1. LWA full antenna aperture (12 waveguides). Total length : 1758 mm. Number of slots: 118. The total breadboard is fabricated by extrusion in two pieces each one containing 6 waveguides.
2. Transitions from waveguide to SMA coaxial (12 x).
3. Termination loads (12 x). Material: Eccosorb MF-117.
4. Single BFN made of laboratory devices: 1 to 12 combiner, cables, variable attenuators and variable phase shifters.
   - 1:12 divider PS12-9 from MCLI.
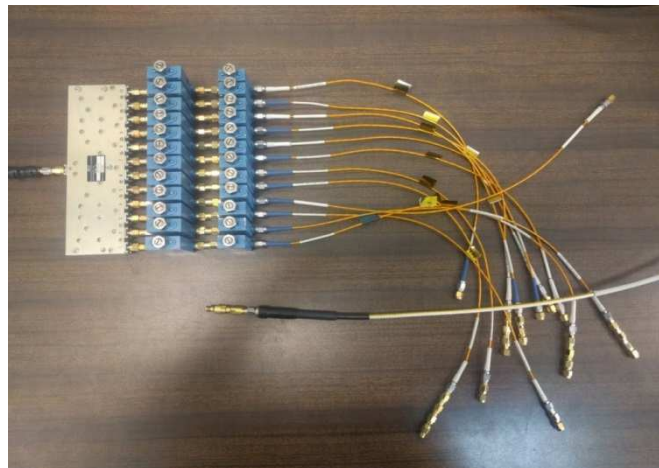
Figure 8.1: BFN

   - Variable attenuators from ARRA (model 6803-20B)
   - Variable phase shifters.
   - Coaxial flexible cables between the different components.
5. Support and attachment pieces for LWA and BFN.

AIRBUS

WAVEMILL

DEFENCE AND SPACE

No.: WAV-TN-ASE-012
Issue: 01 Page: 38
Date: 12/11/2018
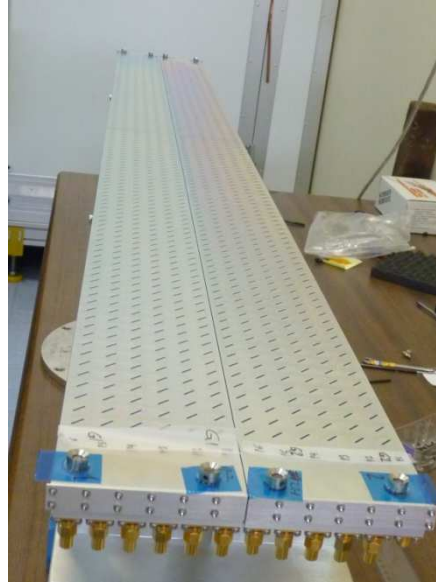
Figure 8.2: BB assembly.

The workshop activities started verifying the waveguides delivered by MIFA. A selection of two in base of better flatness and visual inspection was done. After the total assembly of the BB the DEA measurements and adjustment were done.

AIRBUS

DEFENCE AND SPACE

WAVEMILL

No.:	WAV-TN-ASE-012
Issue:	01 Page: 39
Date:	12/11/2018

9.   BREADBOARD MEASUREMENTS.

9.1   DIMENSIONAL MEASUREMENTS RESULTS

DEA measurements after final adjustment of the waveguides are here below included:

	MEDIDA			NOMINAL			DIF				TOL
	Xant	Yant	Zant	Xant	Yant	Zant	X S/C	Y S/C	Z S/C	XYZ	⊕ ⌀1
	[mm]	[mm]	[mm]	[mm]	[mm]	[mm]	[mm]	[mm]	[mm]	[mm]	
origin	-0,067	-87,014	0,064	0,000	-87,000	0,000	-0,067	-0,014	0,064	0,093	OK
							M	ACOS	ANG		
								rad	o		∠ 0.5
Xher	1,000000	-0,000004	0,000065	1,000000	0,000000	0,000000	1,0000000	0,000	0,004		OK
Yher	0,000004	1,000000	-0,000068	0,000000	1,000000	0,000000	1,0000000	0,000	0,004		OK
Zher	-0,000065	0,000068	1,000000	0,000000	0,000000	1,000000	1,0000000	0,000	0,005		OK

Table 9-1: DEA results

AIRBUS

DEFENCE AND SPACE

No.:	**WAV-TN-ASE-012**		
Issue:	**01**	**Page:**	**40**
Date:	**12/11/2018**		

WAVEMILL

9.2   ON BENCH TESTS (S-PARAMETERS)

Following the test plan RD[12] the S-parameters of all LW have been measured.

Plots below show the matching and coupling measurements obtained after measuring from each connector of each LWs.
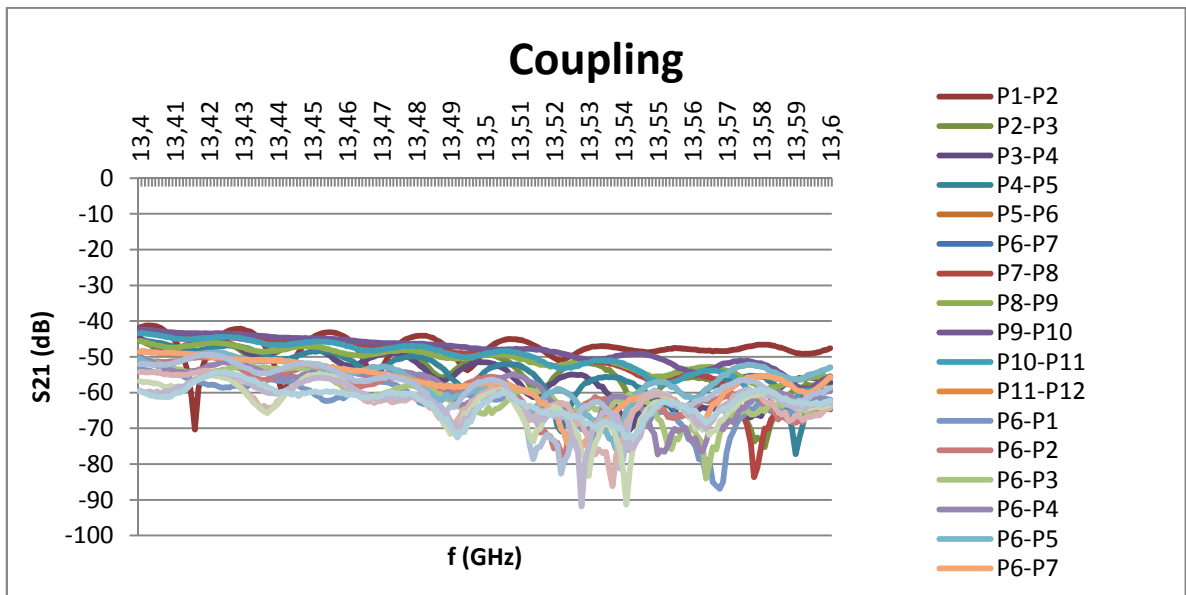
Figure 9.1 Coupling between LWAs

Coupling measured between any LWAs is very low (under -40 dB).

AIRBUS

DEFENCE AND SPACE

WAVEMILL

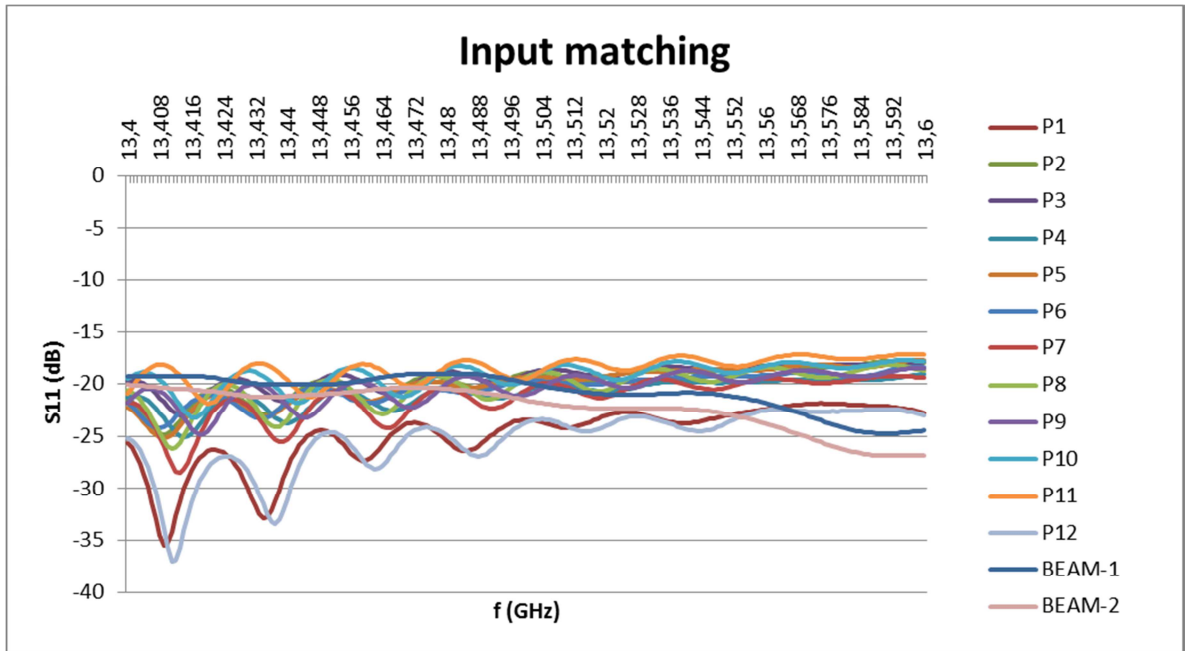| No.:	**WAV-TN-ASE-012**	
Issue:	**01**	**Page: 41**
Date:	**12/11/2018**	

Figure 9.2 Matching of LWs input ports and full BB.

9.3 ON ANECHOIC CHAMBER MEASUREMENTS

Once the BFN has been installed to the backside of the BB the Wavemill breadboard was installed at the positioner in the anechoic chamber.

Figure below shows the Wavemill Breadboard installed on the positioner.

AIRBUS

DEFENCE AND SPACE

WAVEMILL

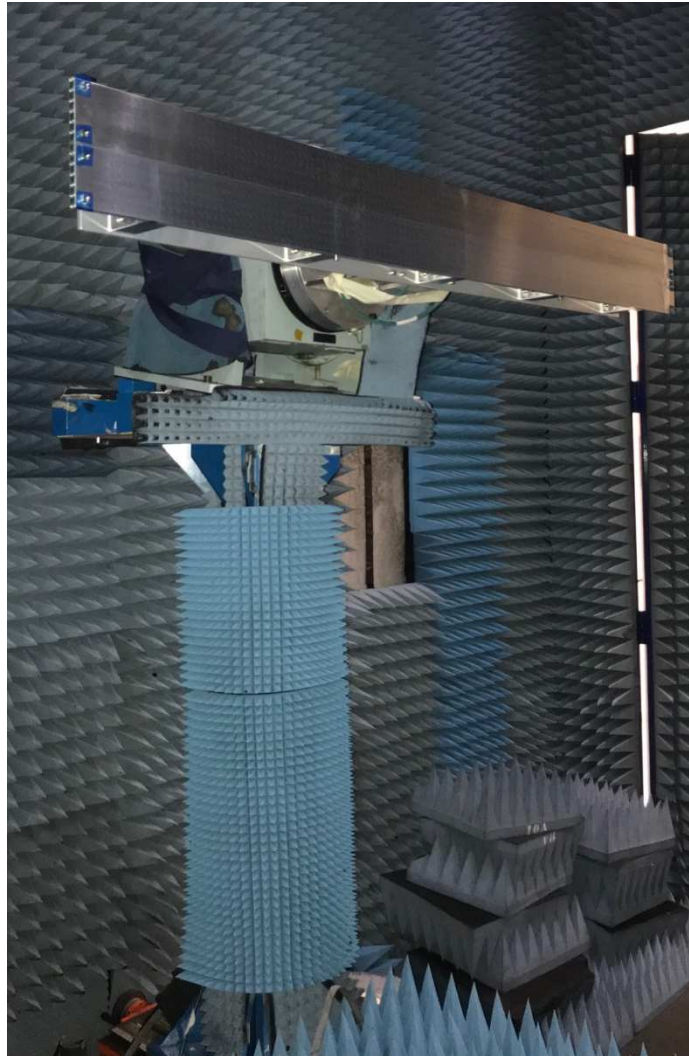| No.: | **WAV-TN-ASE-012** |
| Issue: | **01 Page: 42** |
| Date: | **12/11/2018** |

Figure 9.3 Wavemill Breadboard in the anechoic chamber.

9.3.1 LWA Radiation patterns.

The following plots show the measured radiation patterns of one of the two LWAs tested (LWA-1 at the edge and LWA-6 at the centre) and their comparison with predictions.

Good agreement in radiation patterns between measured and CST simulations is observed in all cases.

AIRBUS

DEFENCE AND SPACE

WAVEMILL

No.:	**WAV-TN-ASE-012**	
Issue:	**01**	**Page: 43**
Date:	**12/11/2018**	

E theta: WAVEMILL BREADBOARD LWA-1 — Measured

E theta: WAVEMILL BB BEAM-1 — Simulated

AIRBUS

DEFENCE AND SPACE

WAVEMILL

No.:	**WAV-TN-ASE-012**
Issue:	**01 Page: 44**
Date:	**12/11/2018**

Figure 9.4 Wavemill LWA-1 measured and predicted radiation patterns (Theta component: E_θ). f=13.50 GHz.

AIRBUS

WAVEMILL

DEFENCE AND SPACE

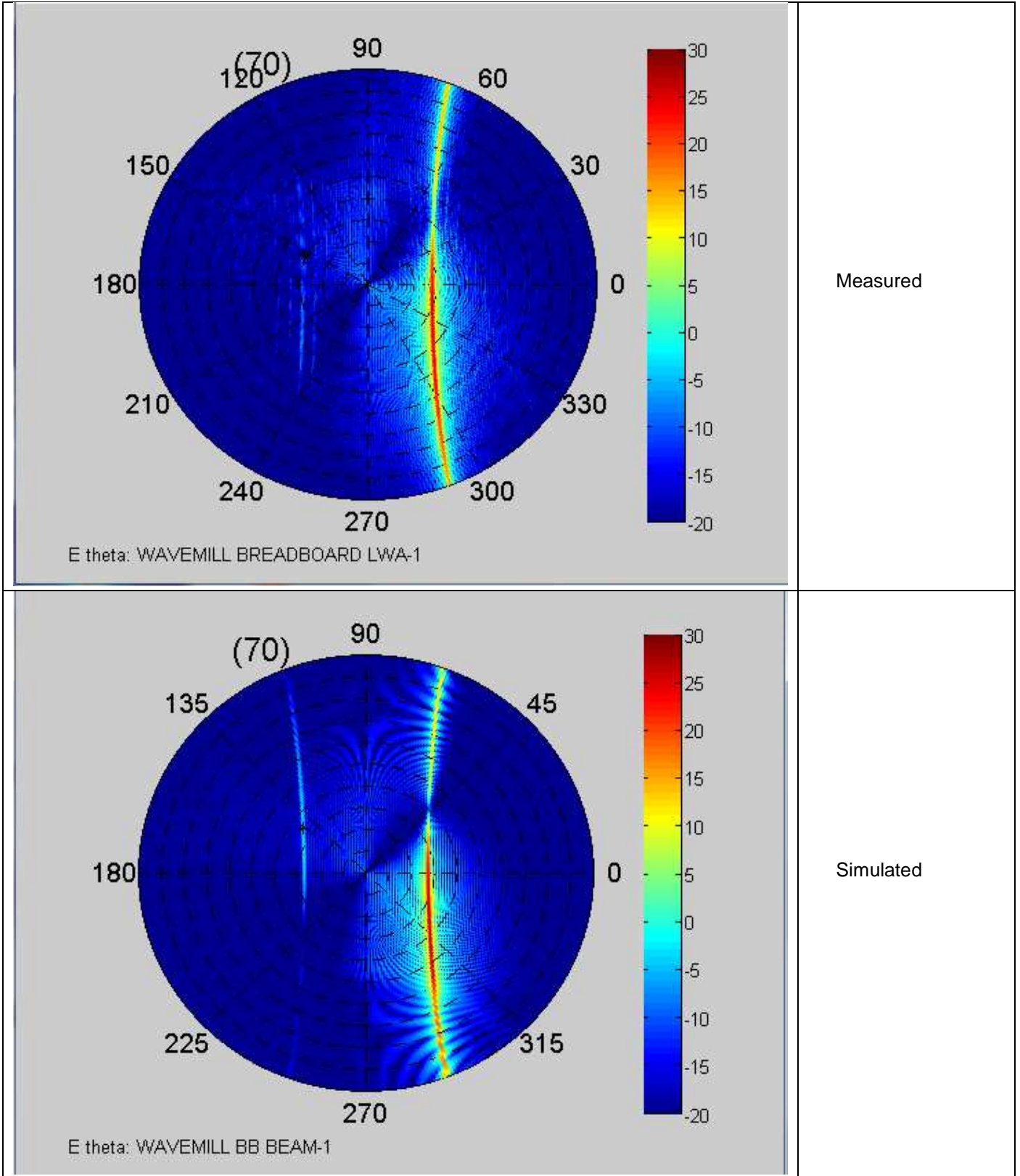| No.:	**WAV-TN-ASE-012**
Issue:	**01 Page: 45**
Date:	**12/11/2018**
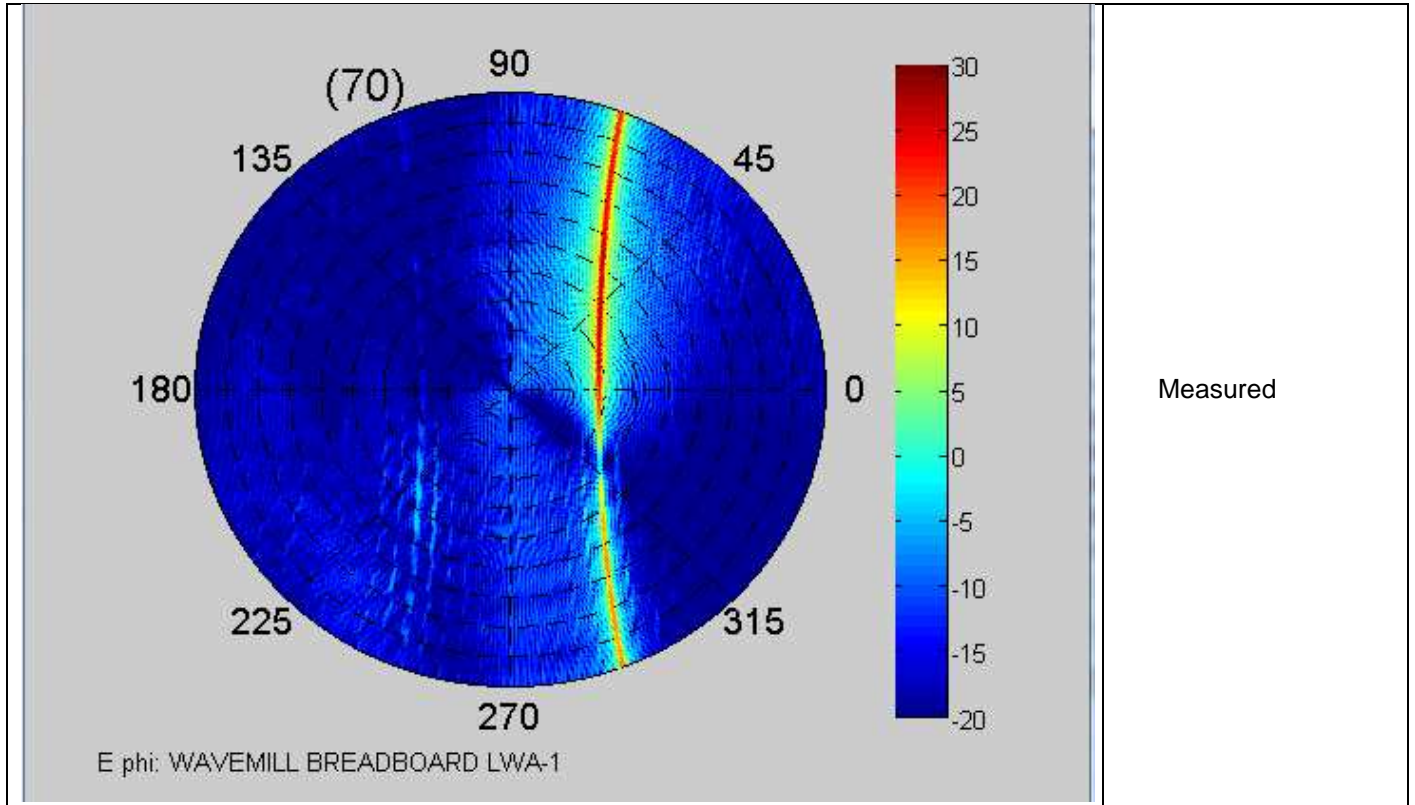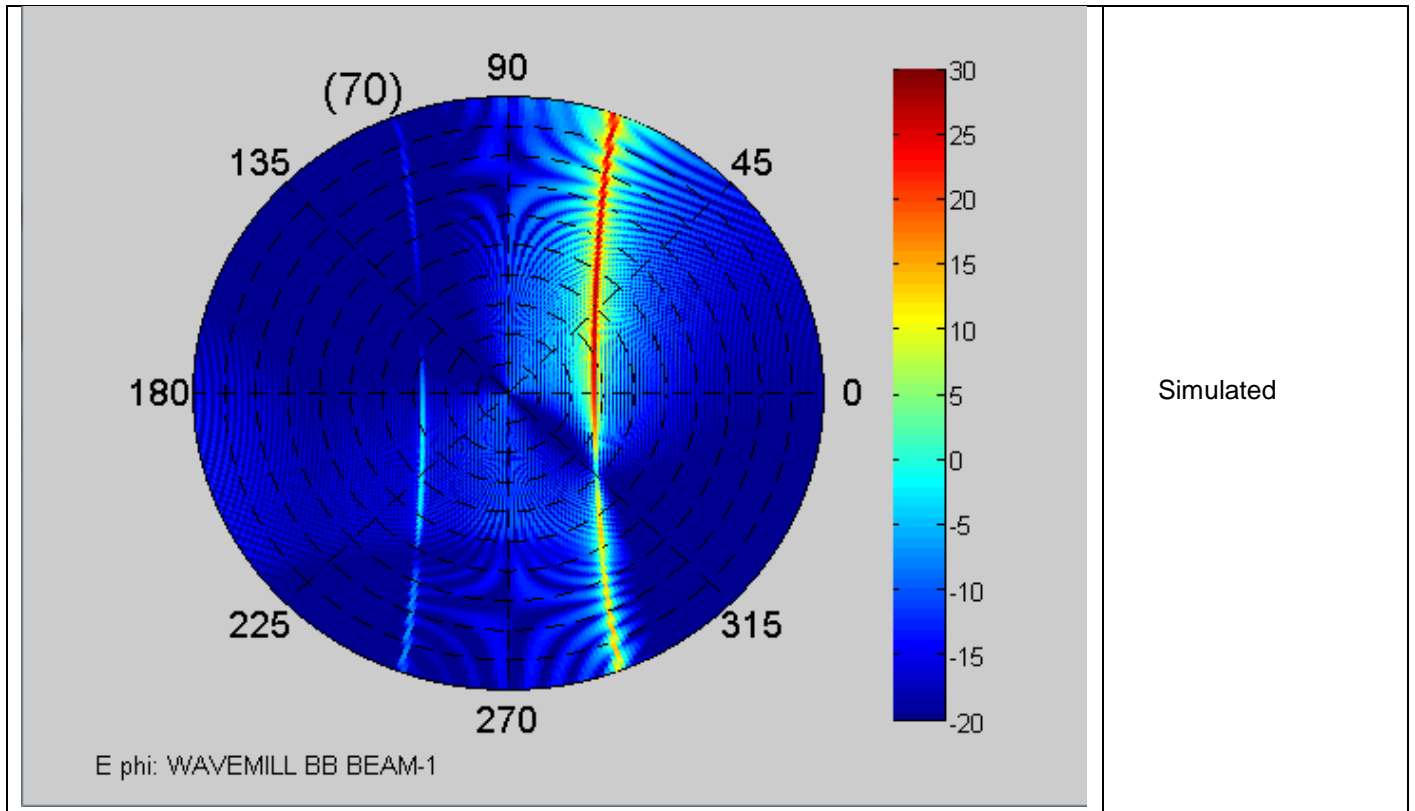
Figure 9.5 Wavemill LWA-1 measured and predicted radiation patterns (Phi component: E_Φ). f=13.50 GHz.

AIRBUS

WAVEMILL

DEFENCE AND SPACE

No.:	**WAV-TN-ASE-012**
Issue:	**01 Page: 46**
Date:	**12/11/2018**

TOTAL FIELD: WAVEMILL BREADBOARD LWA-1

Measured

E total: WAVEMILL BB LWA-1

Simulated
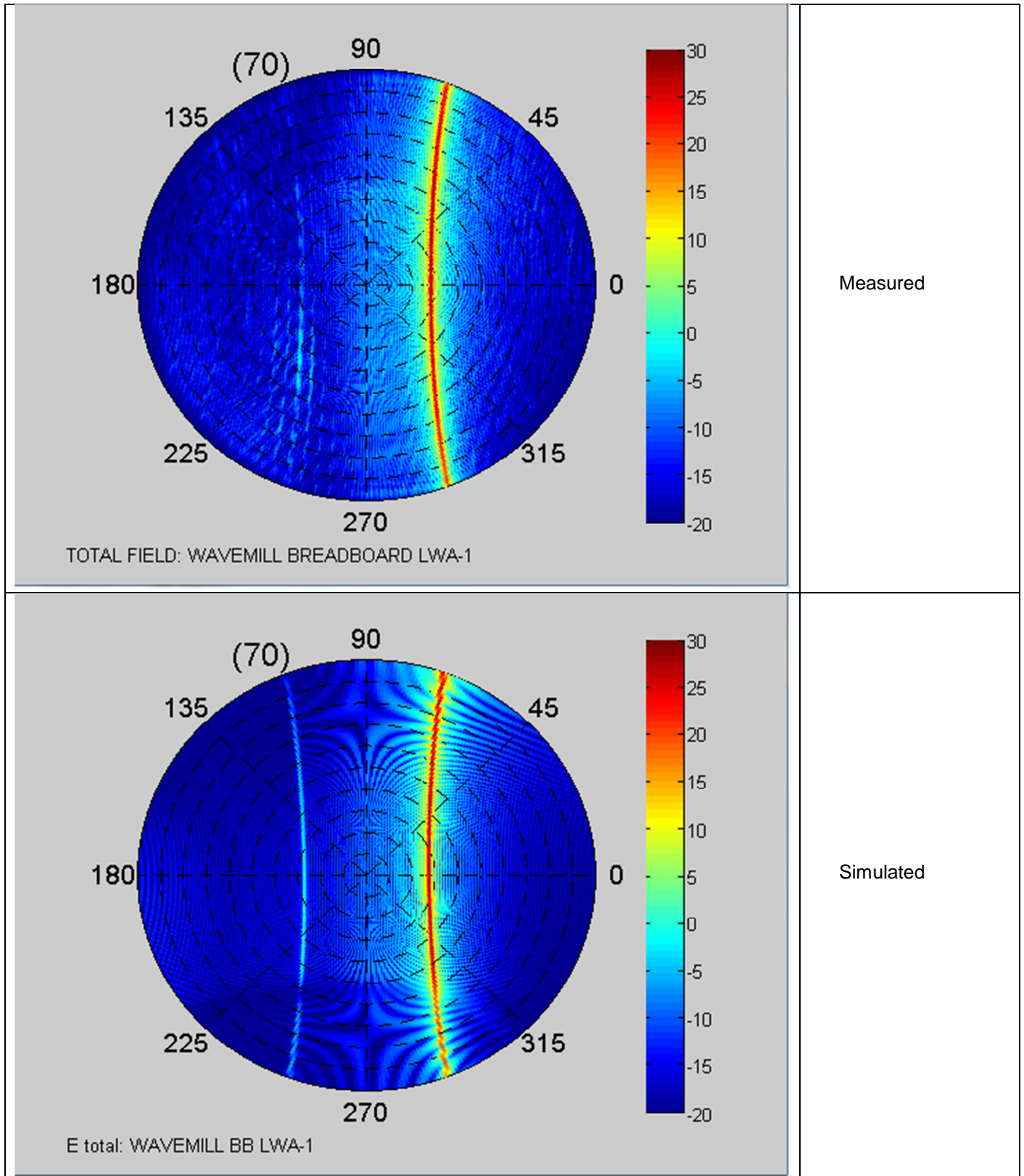
Figure 9.6 Wavemill LWA-1 measured and predicted radiation patterns (Total field). f=13.50 GHz.

Following figure shows the comparison between one LWA (LWA-6) measured and predicted azimuth and elevation plots.
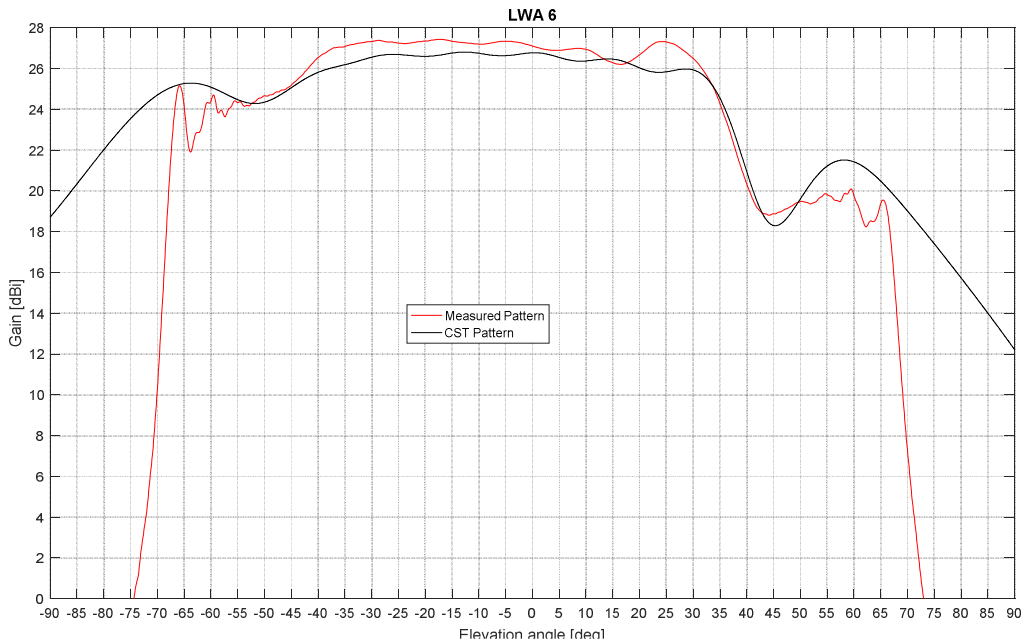

Figure 9.7 Wavemill LWA-6 measured and predicted elevation cuts. f=13.50 GHz.

Table below shows the difference in pointing between measured and predicted azimuth cuts pointing.

LWA-1	Measured Beam pointing [Deg]	Theoretical Beam pointing [Deg]
Azimuth	70.60º	70.98º

LWA-6	Measured Beam pointing [Deg]	Theoretical Beam pointing [Deg]
Azimuth	70.75º	70.98º

Table 9-2. Wavemill Pointing (LWA-1 and LWA-6).

There is some difference in pointing between simulations and measurements and different depending on the concrete LWA. This foreseen effect (due mainly to manufacturing tolerances) can be corrected by proper mechanical tilting.

AIRBUS

DEFENCE AND SPACE

WAVEMILL

No.:	**WAV-TN-ASE-012**	
Issue:	**01**	**Page: 48**
Date:	**12/11/2018**	

The following table shows the comparison between measured and simulated directivities and losses. Very good agreement is obtained regarding directivity and losses.

AIRBUS

WAVEMILL

DEFENCE AND SPACE

No.:	WAV-TN-ASE-012
Issue:	01 Page: 49
Date:	12/11/2018

Directivity (dB)	Measured	Simulated
LWA-1	26.98	26.85
LWA-6	27.49	26.80

Losses (dB)	Measured	Simulated
LWA-1	3.24	3.12
LWA-6	3.08	3.17

Table 9-3. Wavemill Directivity and Losses (LWA-1 and LWA-6).

The difference in the LWA-6 measured directivity (with respect to measurements) is mainly due to integration over a small area in theta (70⁰).

AIRBUS

WAVEMILL

DEFENCE AND SPACE

No.:	**WAV-TN-ASE-012**
Issue:	**01 Page: 50**
Date:	**12/11/2018**

9.3.2   Wavemill Breadboard Radiation patterns.

The following plots show the measured radiation patterns of the two beams tested for the complete breadboard with the BFN and their comparison with predictions.

Good agreement in radiation patterns between measured and CST simulations is observed in all cases.
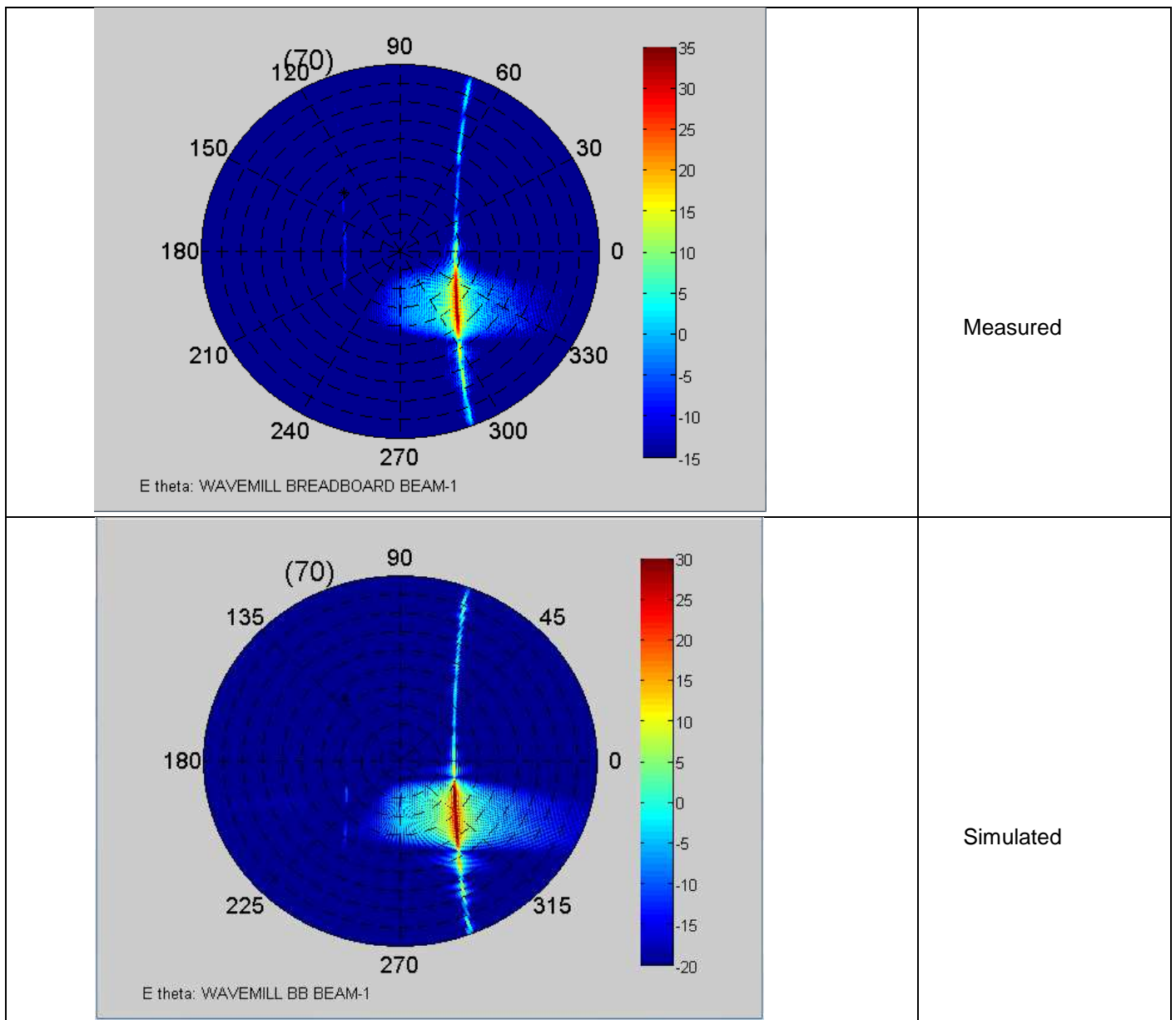
	Measured
	Simulated

Figure 9.8 Wavemill BB BEAM-1 measured and predicted radiation patterns (Theta component: E_θ). f=13.50 GHz.

AIRBUS

DEFENCE AND SPACE

WAVEMILL

No.:	**WAV-TN-ASE-012**
Issue:	**01** Page: **51**
Date:	**12/11/2018**

AIRBUS

DEFENCE AND SPACE

WAVEMILL

No.:	**WAV-TN-ASE-012**
Issue:	**01** Page: **52**
Date:	**12/11/2018**

| | Measured |
| | Simulated |
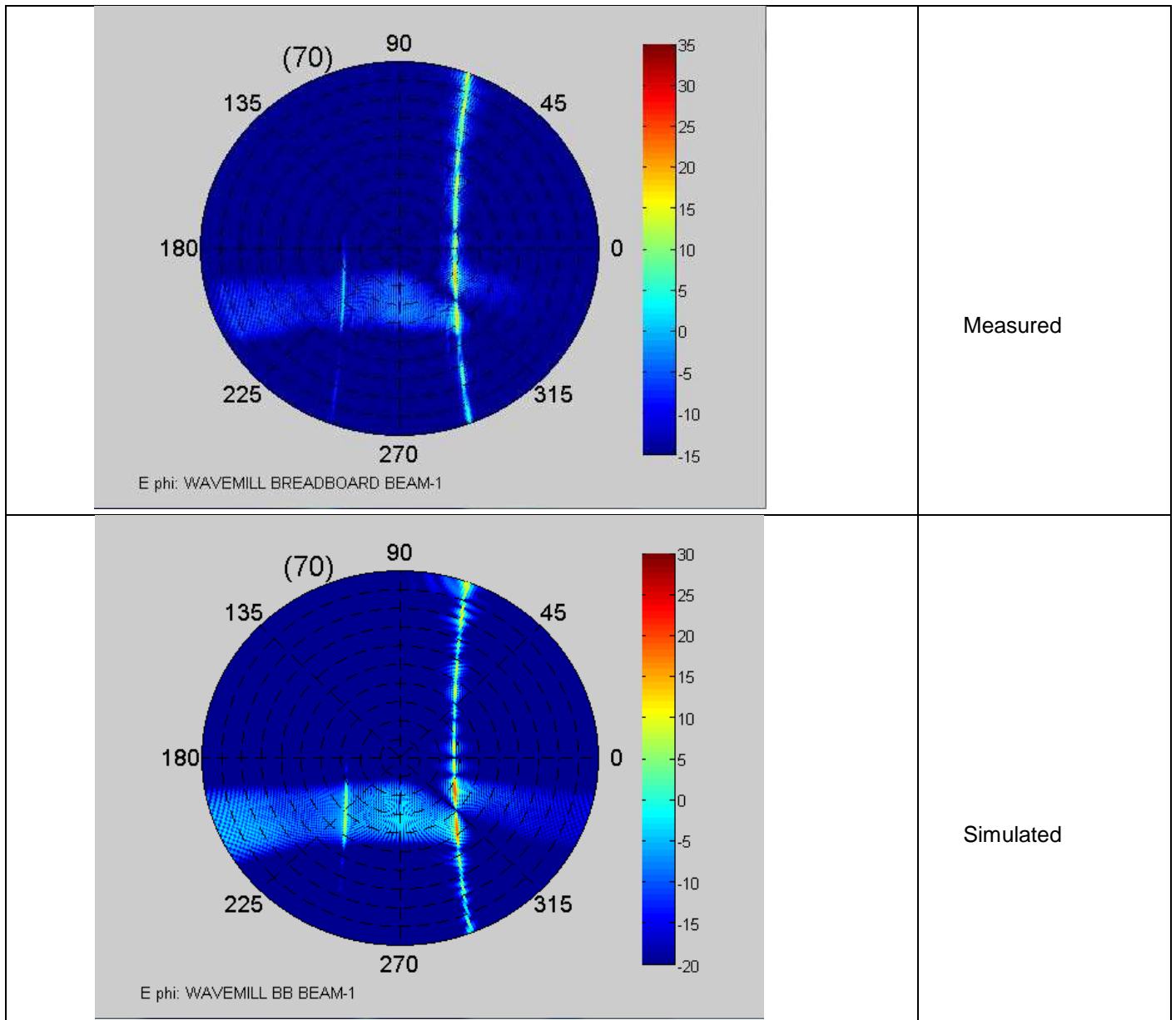
Figure 9.9 Wavemill BB BEAM-1 measured and predicted radiation patterns (Phi component: E_Φ). f=13.50 GHz.

AIRBUS

WAVEMILL

DEFENCE AND SPACE

No.:	**WAV-TN-ASE-012**
Issue:	**01 Page: 53**
Date:	**12/11/2018**

Measured

Simulated
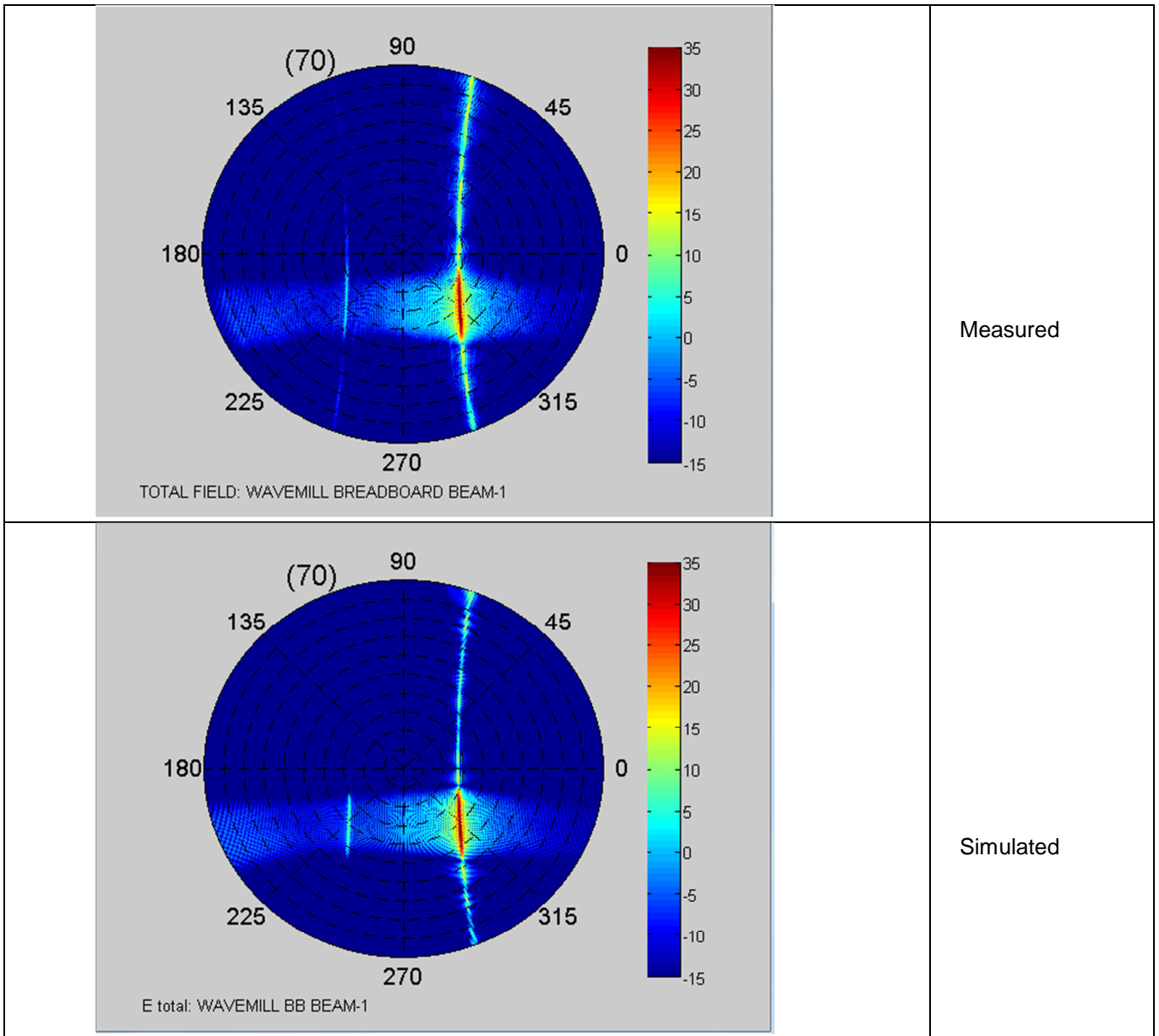
Figure 9.10 Wavemill BB BEAM-1 measured and predicted radiation patterns (Total field). f=13.50 GHz.

AIRBUS

WAVEMILL

DEFENCE AND SPACE

No.:	**WAV-TN-ASE-012**
Issue:	**01** Page: **54**
Date:	**12/11/2018**
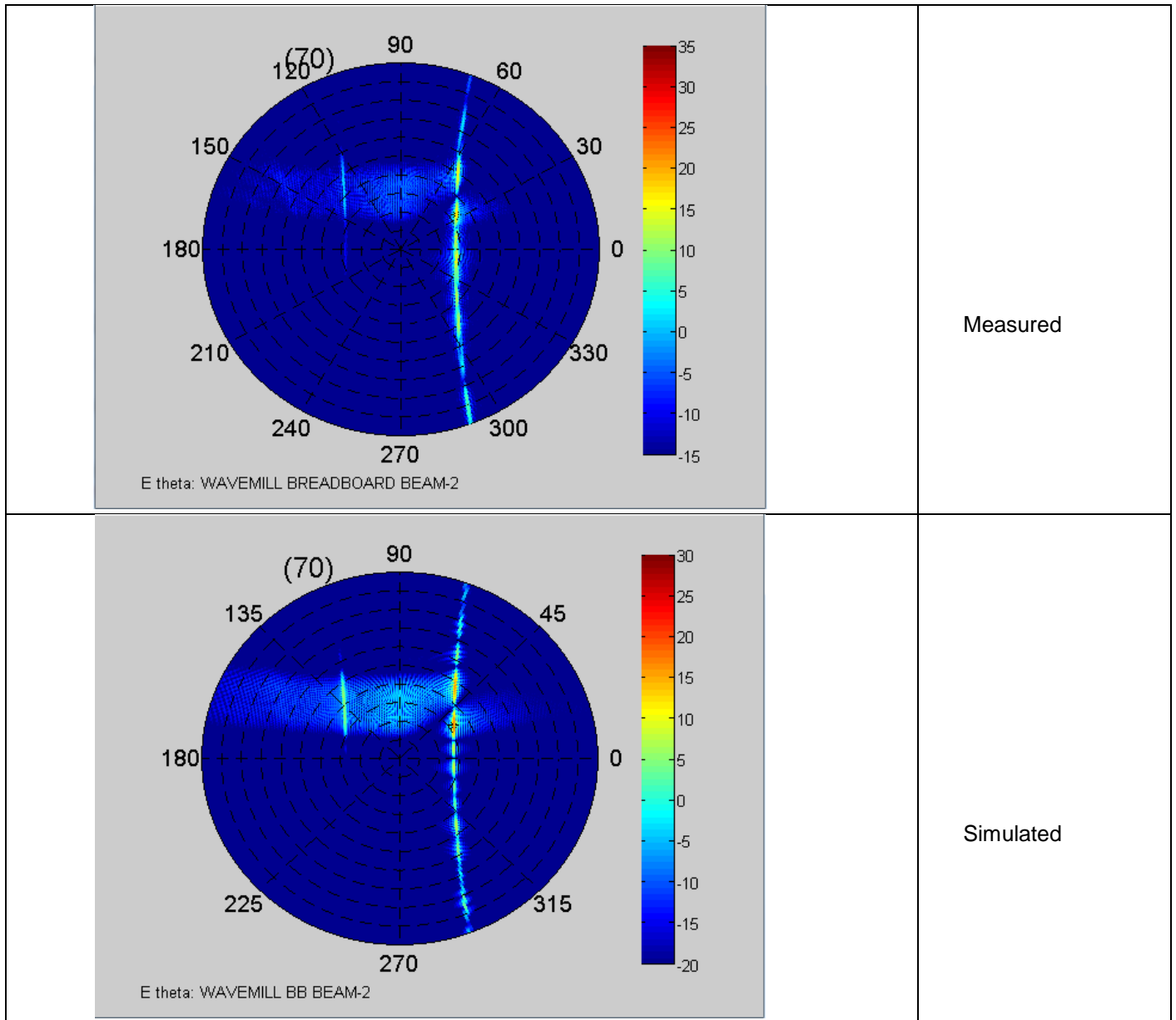
Figure 9.11 Wavemill BB BEAM-2 measured and predicted radiation patterns (Theta component: E_θ). f=13.50 GHz.

AIRBUS

DEFENCE AND SPACE

WAVEMILL

No.:	**WAV-TN-ASE-012**
Issue:	**01 Page: 55**
Date:	**12/11/2018**
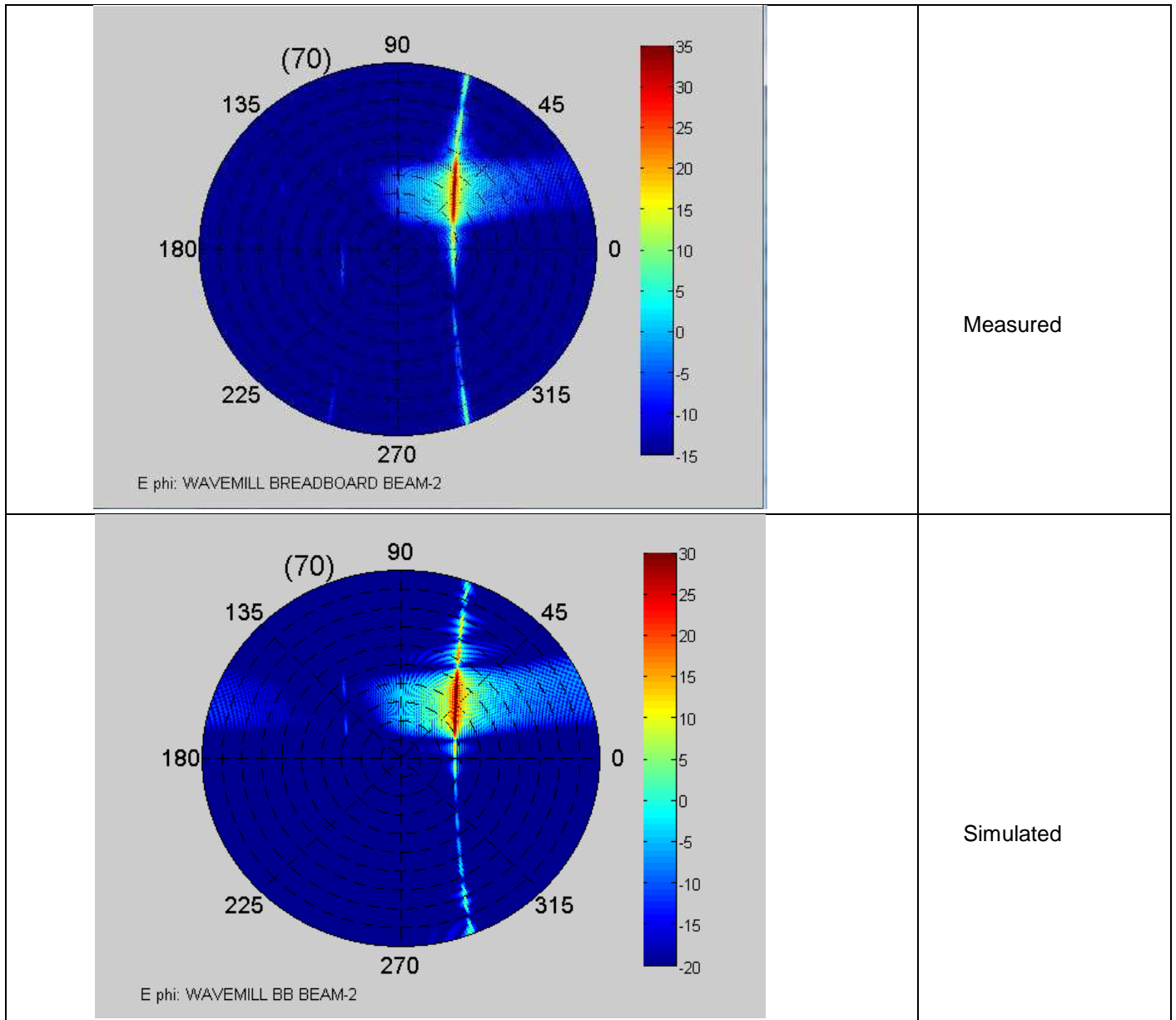
Figure 9.12 Wavemill BB BEAM-2 measured and predicted radiation patterns (Phi component: E_ϕ). f=13.50 GHz.

AIRBUS

WAVEMILL

DEFENCE AND SPACE

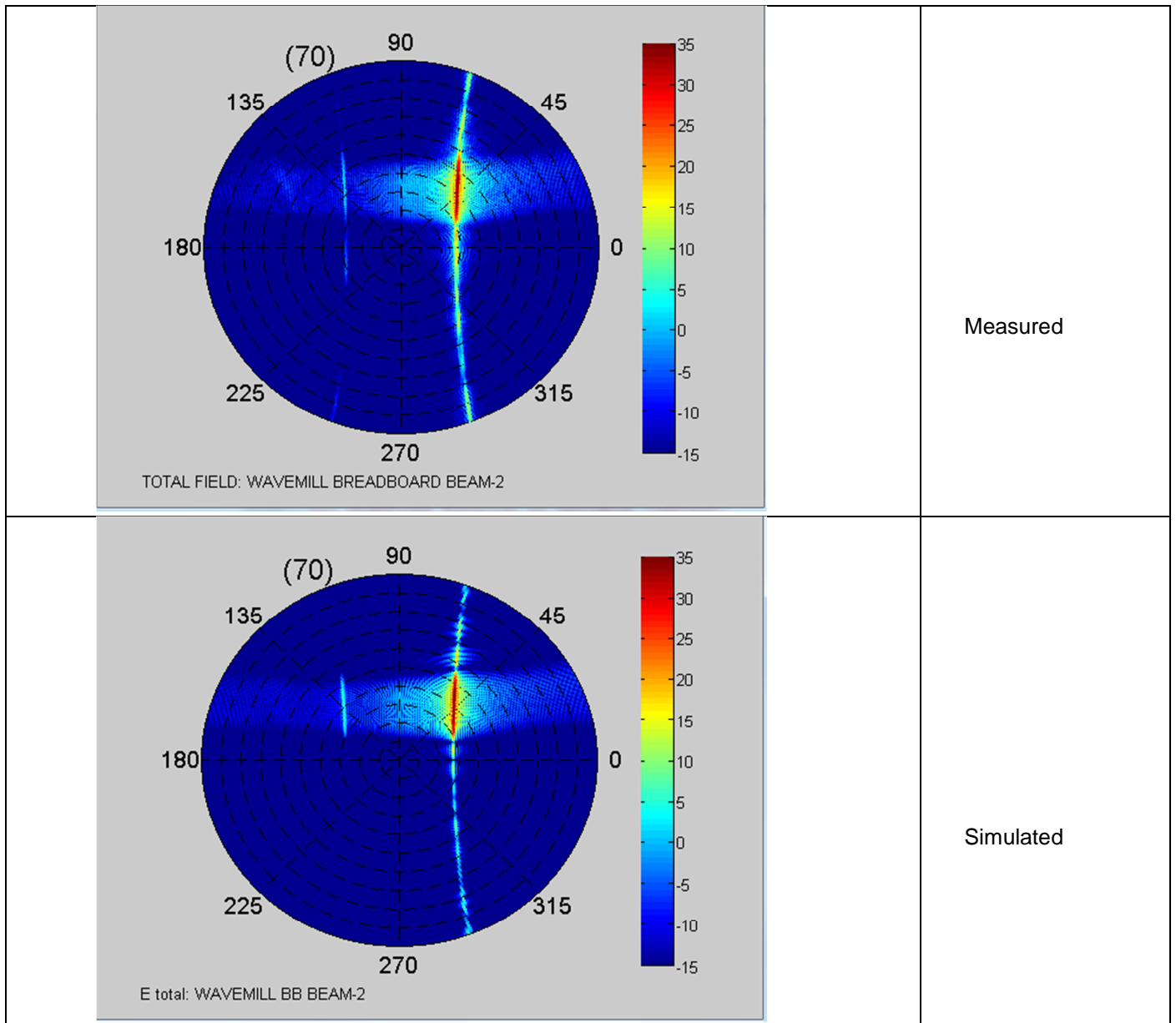| No.:	**WAV-TN-ASE-012**		
Issue:	**01**	Page:	**56**
Date:	**12/11/2018**		

Figure 9.13 Wavemill BB BEAM-2 measured and predicted radiation patterns (Total field). f=13.50 GHz.

Following figure shows the comparison between measured and predicted azimuth and elevation plots. Azimuth sidelobes are always better than 13 dB (requirement greater than 10 dB).
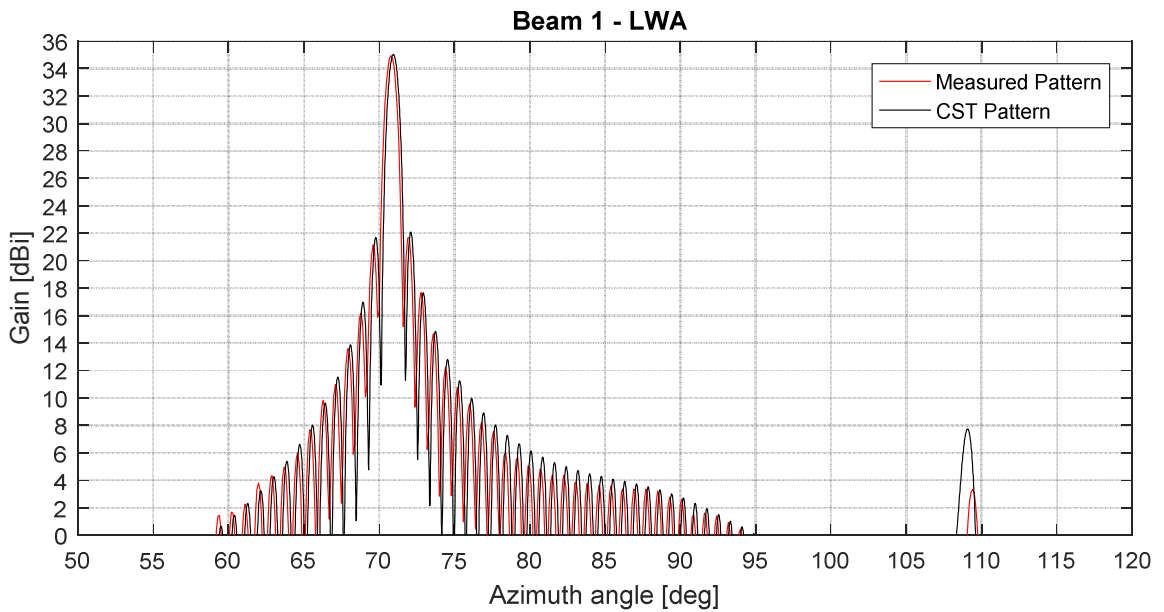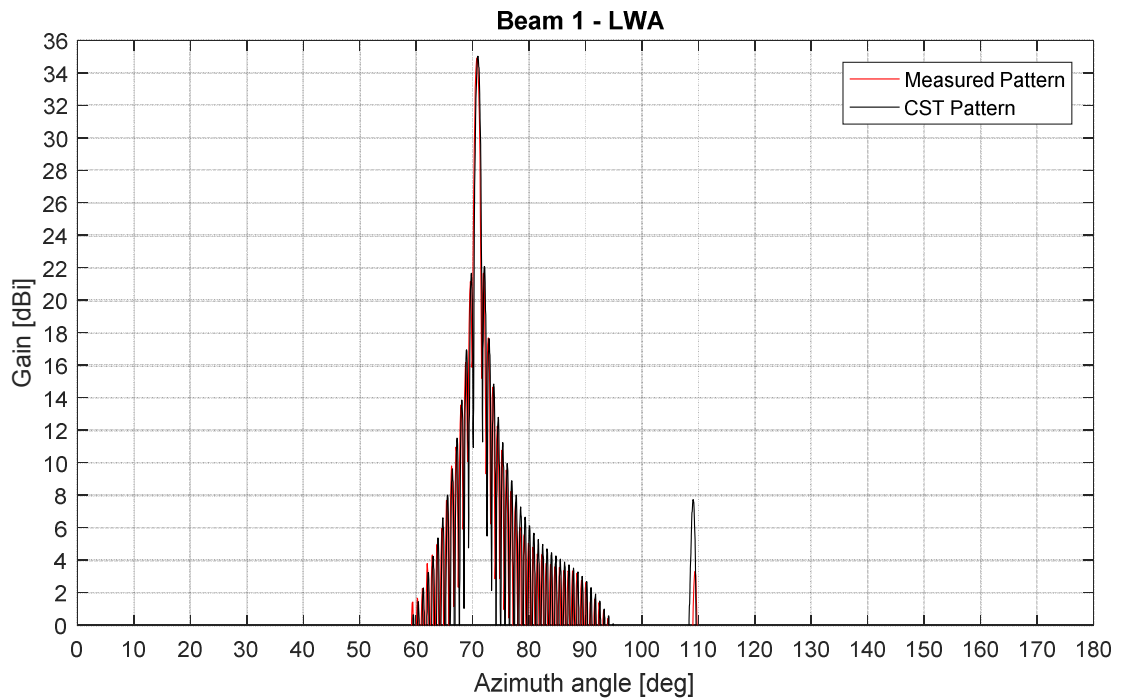
AIRBUS

DEFENCE AND SPACE

WAVEMILL

No.:	**WAV-TN-ASE-012**	
Issue:	**01**	Page: **57**
Date:	**12/11/2018**	

Figure 9.14 Wavemill BB Beam-1 measured and predicted azimuth cuts. f=13.50 GHz.

AIRBUS

DEFENCE AND SPACE

WAVEMILL

No.:	**WAV-TN-ASE-012**
Issue:	**01 Page: 58**
Date:	**12/11/2018**

Beam 1 - LWA
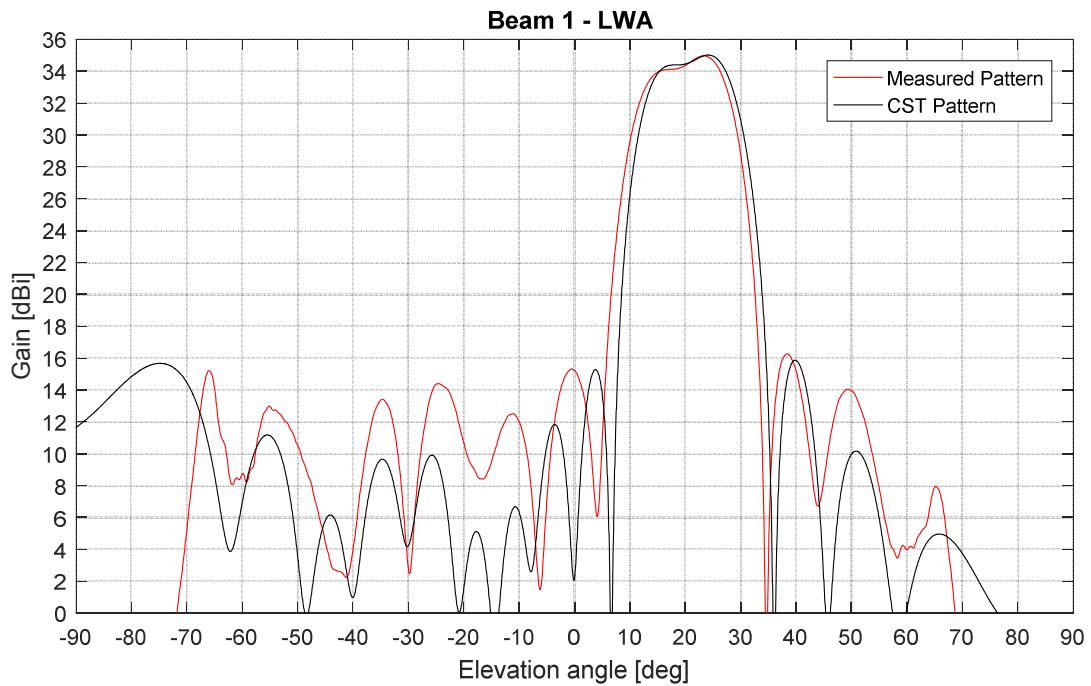
Figure 9.15 Wavemill BB Beam-1 measured and predicted elevation cuts. f=13.50 GHz.

Beam 2 - LWA

AIRBUS

WAVEMILL

DEFENCE AND SPACE

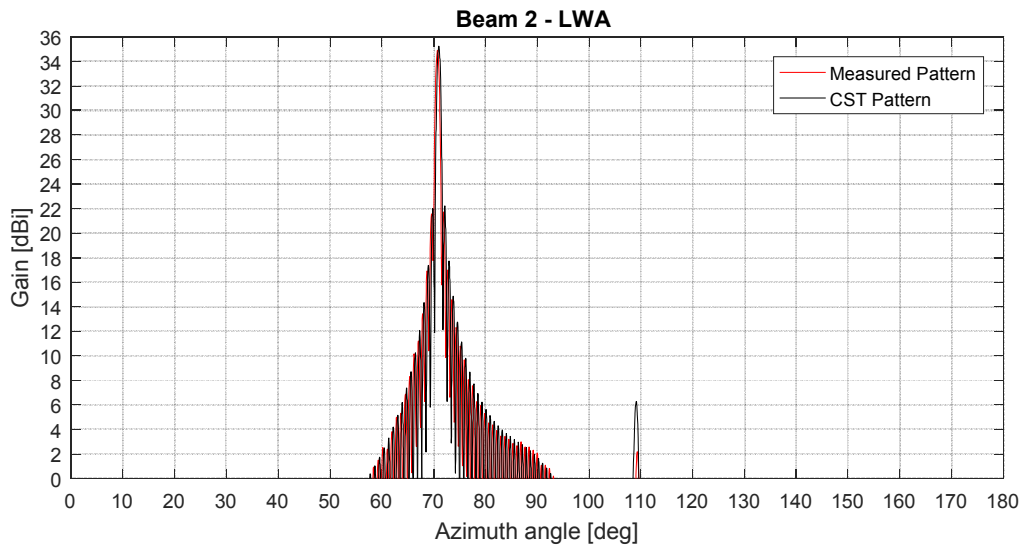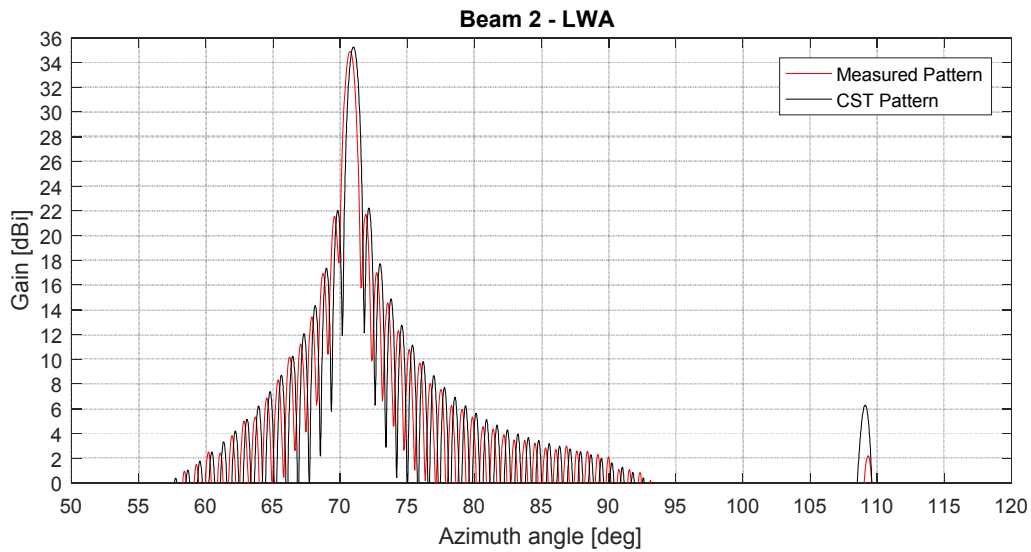| No.: | **WAV-TN-ASE-012** |
| Issue: | **01 Page: 59** |
| Date: | **12/11/2018** |

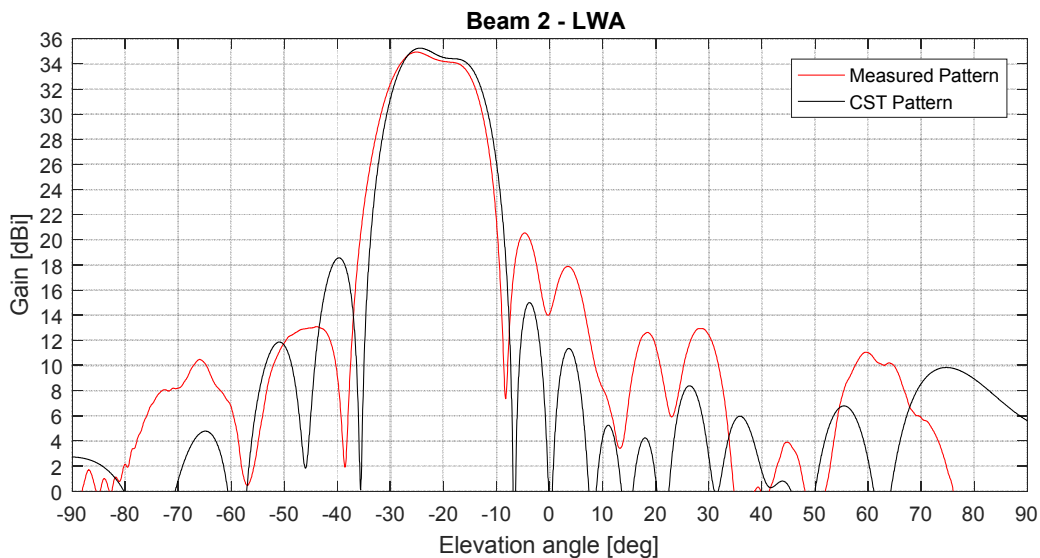**Figure 9.16 Wavemill BB Beam-2 measured and predicted azimuth cuts. f=13.50 GHz.**

Figure 9.17 Wavemill BB Beam-2 measured and predicted elevation cuts. f=13.50 GHz.

Table below shows the difference in pointing between measured and predicted azimuth cuts pointing.

Beam-1	**Measured Beam pointing [Deg]**	**Theoretical Beam pointing [Deg]**
Azimuth	70.825º	70.94º

AIRBUS

DEFENCE AND SPACE

WAVEMILL

No.:	WAV-TN-ASE-012
Issue:	01 Page: 60
Date:	12/11/2018

Beam-2	Measured Beam pointing [Deg]	Theoretical Beam pointing [Deg]
Azimuth	70.75º	70.99º

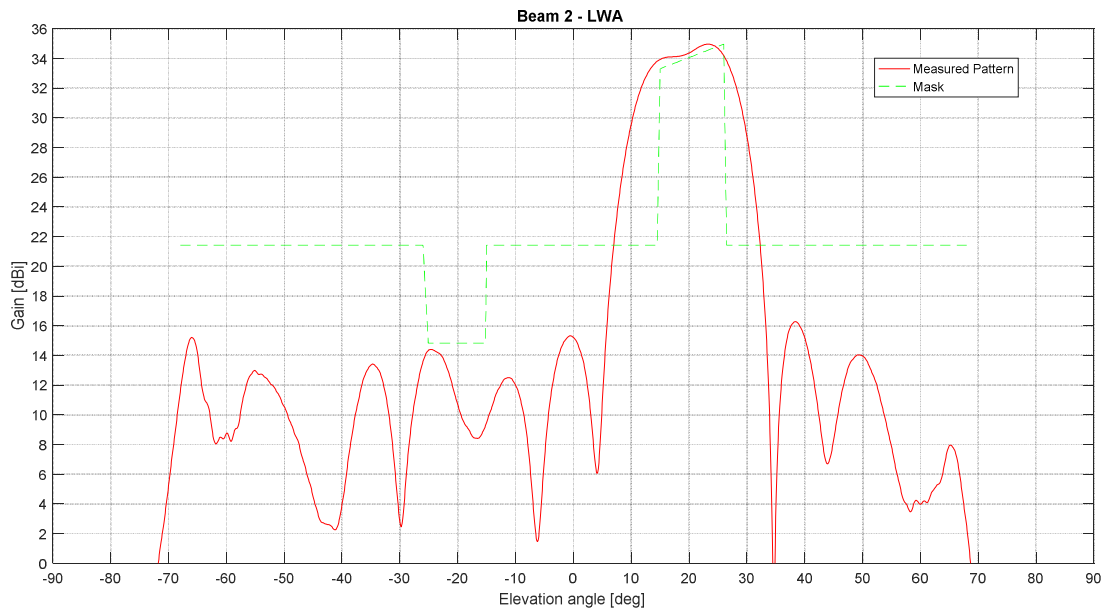**Table 9-4. Wavemill BB azimuth pointing (Beam-1 and Beam-2).**

There is some difference in pointing between simulations and measurements (around 0.11º for Beam-1 and 0.24º for Beam-2). This foreseen effect (due mainly to manufacturing tolerances) can be partially corrected with proper mechanical tilting.

The following table shows the comparison between measured and simulated directivities. Very good agreement is obtained regarding directivity.

Directivity (dB)	Measured	Simulated
Beam-1	34.96	35.02
Beam-2	34.93	35.24

Table 9-5. Wavemill Directivity and Losses (BB Beam-1 and Beam-2).

Following figures show the measured elevation cuts for both beam versus the requirement mask. Sidelobes mask in compliant for both measured beams even for the reverse side lobe.

Figure 9.18 Wavemill BB Beam-1 measured elevation cut vs requirement mask. f=13.50 GHz.

AIRBUS

DEFENCE AND SPACE

WAVEMILL

No.:	**WAV-TN-ASE-012**
Issue:	**01 Page: 61**
Date:	**12/11/2018**
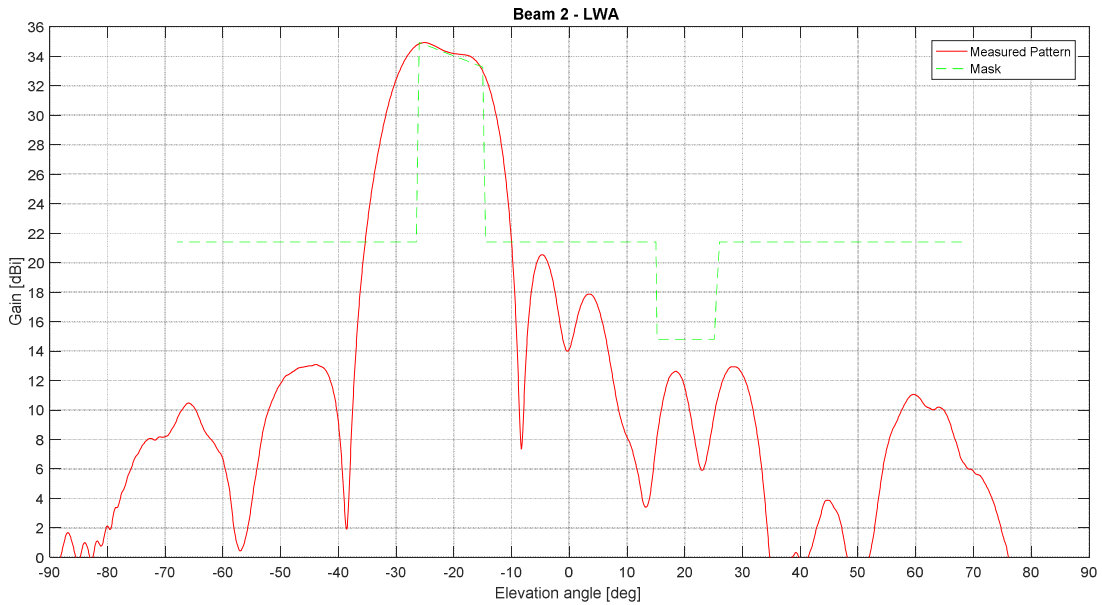
**Figure 9.19 Wavemill BB Beam-2 measured elevation cut vs requirement mask.
f=13.50 GHz.**

Main beam elevation cuts show small non-compliance of 0.40 dB for Beam 1 and 0.45 dB for Beam 2.

If a rotation of 0.8º is applied in the elevation plane for both beams (mechanical tilting) an almost compliant elevation cut is obtained (NC of only 0.10 dB for Beam 1 and 0.14 dB for Beam 2). See **Figure 9.20** and **Figure 9.21**.
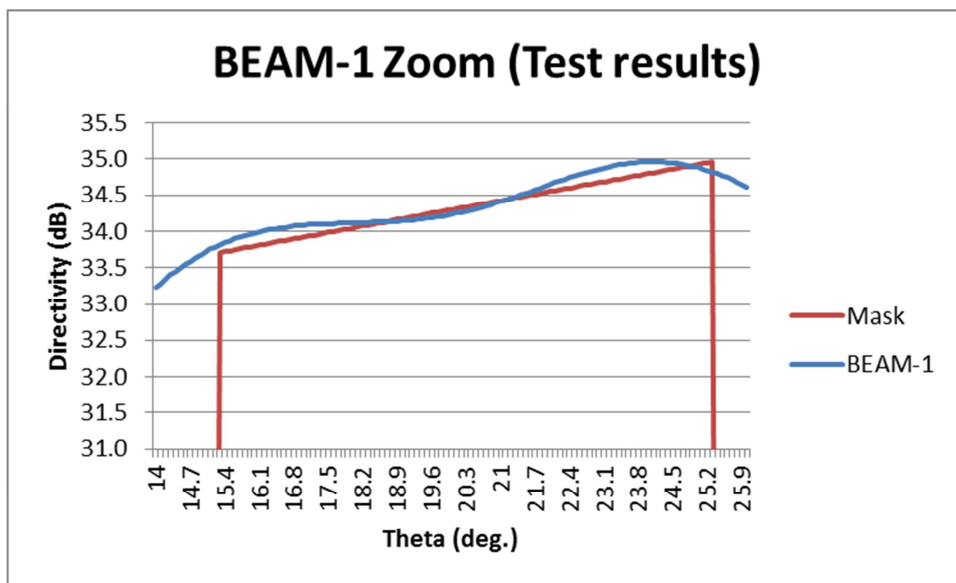
AIRBUS

WAVEMILL

DEFENCE AND SPACE

No.:	**WAV-TN-ASE-012**
Issue:	**01 Page: 62**
Date:	**12/11/2018**

Figure 9.20 Wavemill BB Beam-1 measured elevation cut vs requirement mask.
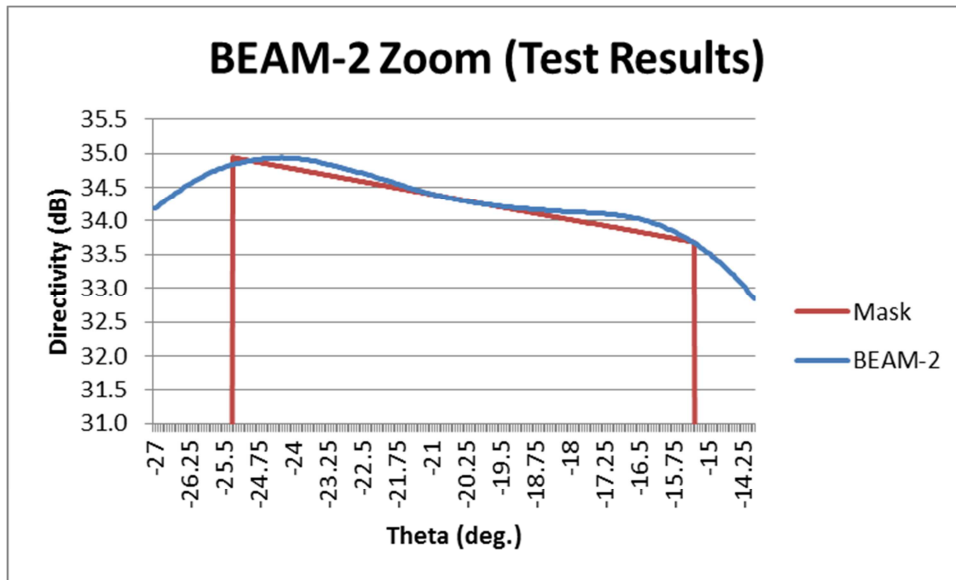**f=13.50 GHz. Zoom. Rotation of 0.8⁰ in the elevation plane.**

Figure 9.21 Wavemill BB Beam-2 measured elevation cut vs requirement mask.
f=13.50 GHz. Zoom. Rotation of 0.8⁰ in the elevation plane.

AIRBUS

WAVEMILL

DEFENCE AND SPACE

No.:	WAV-TN-ASE-012
Issue:	01 Page: 63
Date:	12/11/2018

10. CONCLUSIONS

Test results of the representative antenna breadboard allow stating a good agreement between predictions and measurements and to assess the adequacy of the design to Wavemill mission needs. Comparison with requirements has also been performed showing close to compliance performance.

Some performances obtained during this development could be improved with a more detailed antenna design as for the case of the azimuth co-alignment that could be significantly improved with a more accurate thermo-elastic analysis and design.

AIRBUS

WAVEMILL

DEFENCE AND SPACE

No.: WAV-TN-ASE-012
Issue: 01 **Page:** 64
Date: 12/11/2018

END OF DOCUMENT